2. Miyawaki T, Hirata M, Moriyama K, et al. Metabolic syndrome in Japanese diagnosed with visceral fat measurement by computed tomography. *Proc Jpn Acad Ser B* 2005;81:471-479.
3. Després JP, Lemieux I. Abdominal obesity and metabolic syndrome. *Nature* 2006; 444:881-887.
4. Ferland M, Després JP, Trembly A, et al. Assessment of adipose tissue distribution by computed axial tomography in obese women: association with body density and anthropometric measurements. *Br J Nutr* 1989;61:139-148.
5. Kuk JL, Lee S, Heymsfield SB, Ross R. Waist circumference and abdominal adipose tissue distribution: influence of age and sex. *Am J Clin Nutr* 2005;81: 1330-1334.
6. Cornier MA, Després JP, Davis N, et al. A scientific statement from the American Heart Association. *Circulation* 2011;124:1996-2019.
7. Miyawaki T, Abe M, Yahata K, Kajiyama N, Katsuma H, Saito N. Contribution of visceral fat accumulation to the risk factors for atherosclerosis in non-obese Japanese. *Intern Med* 2004;43:1138-1144.
8. Isbess JM, Tamboli RA, Hansen EN, et al. The importance of caloric restriction in the early improvements in insulin sensitivity after Roux-en Y gastric bypass surgery. *Diabetes Care* 2010;33:1438-1442.
9. Ryo M, Maeda K, Onda T, et al. A new simple method for the measurement of visceral fat accumulation by bioelectrical impedance. *Diabetes Care* 2005;8:451-453.
10. Nagai M, Komiya H, Mori Y, Ohta T, Kasahara Y, Ikeda Y. Development of a new method for estimating visceral fat area with multi-frequency bioelectrical impedance. *Tohoku J Exp Med* 2008;214:105-112.
11. Shiga T, Oshima Y, Kanai H, Hirata M, Hosoda K, Nakao K. *A simple measurement method of visceral fat accumulation by bioelectrical impedance analysis*, In: *IFMBE Proceedings*, Vol. 17/14: 13th International Conference on Electrical Bioimpedance and the 8th Conference on Electrical Impedance Tomography; Scharfetter H, et al., eds., Springer-Verlag; 2007, pp 687-690.Available at: http://link.springer.com/chapter/10.1007%2F978-3-540-73841-1_177?LI=true.
12. Yoneda M, Tasaki H, Tsuchiya N, et al. A study of bioelectrical impedance analysis methods for practical visceral fat estimation. In: IEEE International Conference on Granular Computing (GCR 2007), Lin TY, et al., eds., IEEE Computer Society Press; 2007, pp 622-627. Available at: http://ieeexplore.ieee.org/xpl/login.jsp?tp=&arnumber=4403174&url=http%3A%2F%2Fieeexplore.ieee.org%2Fxpls%2Fabs_all.jsp%3Farnumber%3D4403174.
13. Shiga T, Hamaguchi T, Oshima Y, et al. *A new simple measurement system of visceral fat accumulation by bioelectrical impedance analysis*. In *IFMBE Proceedings* Vol. 25/7: World Congress on Medical Physics and Biomedical Engineering, Döossel O, et al., eds., Springer-Verlag; 2009, pp 338-341.
14. Matsuzawa Y. Metabolic syndrome—definition and diagnostic criteria in Japan. *J Atheroscler Thromb* 2005;12:301.
15. Li Y, Bujo H, Takahashi K, et al. Visceral Fat: higher responsiveness of fat mass and gene expression to calorie restriction than subcutaneous fat. *Exp Biol Med (Maywood)* 2003;228:1118-1123.
16. Colles SL, Dixon JB, Marks P, et al. Preoperative weight loss with a very-low-energy diet: quantitation of changes in liver and abdominal fat by serial imaging. *Am J Clin Nutr* 2006;84:304-311.

Intracerebroventricular Administration of C-Type Natriuretic Peptide Suppresses Food Intake via Activation of the Melanocortin System in Mice

Nobuko Yamada-Goto,[1] Goro Katsuura,[1] Ken Ebihara,[1] Megumi Inuzuka,[1] Yukari Ochi,[1] Yui Yamashita,[1] Toru Kusakabe,[1] Akihiro Yasoda,[1] Noriko Satoh-Asahara,[2] Hiroyuki Ariyasu,[1] Kiminori Hosoda,[1] and Kazuwa Nakao[1]

C-type natriuretic peptide (CNP) and its receptor are abundantly distributed in the brain, especially in the arcuate nucleus (ARC) of the hypothalamus associated with regulating energy homeostasis. To elucidate the possible involvement of CNP in energy regulation, we examined the effects of intracerebroventricular administration of CNP on food intake in mice. The intracerebroventricular administration of CNP-22 and CNP-53 significantly suppressed food intake on 4-h refeeding after 48-h fasting. Next, intracerebroventricular administration of CNP-22 and CNP-53 significantly decreased nocturnal food intake. The increment of food intake induced by neuropeptide Y and ghrelin was markedly suppressed by intracerebroventricular administration of CNP-22 and CNP-53. When SHU9119, an antagonist for melanocortin-3 and melanocortin-4 receptors, was coadministered with CNP-53, the suppressive effect of CNP-53 on refeeding after 48-h fasting was significantly attenuated by SHU9119. Immunohistochemical analysis revealed that intracerebroventricular administration of CNP-53 markedly increased the number of c-Fos–positive cells in the ARC, paraventricular nucleus, dorsomedial hypothalamus, ventromedial hypothalamic nucleus, and lateral hypothalamus. In particular, c-Fos–positive cells in the ARC after intracerebroventricular administration of CNP-53 were coexpressed with α-melanocyte–stimulating hormone immunoreactivity. These results indicated that intracerebroventricular administration of CNP induces an anorexigenic action, in part, via activation of the melanocortin system. ***Diabetes* 62:1500–1504, 2013**

C-type natriuretic peptide (CNP) is a member of the natriuretic peptide family and has been demonstrated to be abundantly present in the brain, interestingly in discrete hypothalamic areas, such as the arcuate nucleus (ARC) of the hypothalamus, that play pivotal roles in energy regulation (1–3). Two predominant molecular forms of CNP in the porcine brain were reported to be a 22-residue peptide (CNP-22) and its *N*-terminally elongated 53-residue peptide (CNP-53) (1). Moreover, natriuretic peptide receptor-B (NPR-B), a CNP receptor, is also widely distributed in the brain and is reported to be abundantly expressed in the ARC of the hypothalamus (4,5). These findings indicate the possibility that the brain CNP/NPR-B system may regulate energy homeostasis.

In the current study, we examined the effects of intracerebroventricular administration of CNP on food intake induced by refeeding after fasting and by orexigenic peptides, such as neuropeptide Y (NPY) and ghrelin. Also, we examined the involvement of the melanocortin system in the CNP actions.

RESEARCH DESIGN AND METHODS

Animals and diets. Male C57BL/6J mice (6 weeks old) obtained from Japan SLC (Shizuoka, Japan) were housed in plastic cages in a room kept at a room temperature of 23 ± 1°C and a 12:12-h light–dark cycle (lights turned on at 9:00 A.M.). The mice had ad libitum access to water and food (CE-2; CLEA Japan, Tokyo, Japan). All experiments were performed at 10 weeks of age in accordance with the guidelines established by the Institutional Animal Investigation Committee at Kyoto University and the United States National Institutes of Health Guide for the Care and Use of Laboratory Animals. Every effort was made to optimize comfort and to minimize the use of animals.

Peptides. CNP-22, CNP-53, ghrelin, and NPY were purchased from Peptide Institute (Osaka, Japan). SHU9119 was purchased from Bachem AG (Bubendorf, Switzerland).

Intracerebroventricular injection. Intracerebroventricular injection was performed according to our previous report (6).

Measurement of food intake

Fasting-refeeding. Mice were fasted for 48 h and then refed for 4 h. Water was available ad libitum during the experiments. The intracerebroventricular or intraperitoneal administration of CNP-22 or CNP-53 was performed just before refeeding. Food intake was measured for 4 h of refeeding. At the end of experiments, the hypothalamus was collected for examination of the expressions of mRNA for neuropeptides (7).

Nocturnal food intake. To assess the effect of intracerebroventricular administration of CNP-22 or CNP-53 on nocturnal food intake, peptides were injected intracerebroventricularly 1 h before the beginning of the dark phase. Food intake was measured for 15 h after intracerebroventricular injection. Water was available ad libitum during the experiments.

Food intake induced by NPY and ghrelin. The experiments were performed from 11:00 A.M. to 3:00 P.M. CNP-22 or CNP-53 was intracerebroventricularly administrated just before intracerebroventricular injection of NPY (5 nmol/mouse) or intraperitoneal injection of ghrelin (100 nmol/kg). Food intake was measured for 4 h after peptide injection. In these experiments, food and water were available ad libitum.

PCR. The extraction of mRNA and quantitative real-time RT-PCR were performed according to our previous report (8). Primers for preopiomelanocortin, cocaine and amphetamine-related peptide, *NPY*, agouti gene-related peptide (*AgRP*) and glyceraldehyde 3-phosphate dehydrogenase are shown in Supplementary Table 1.

Immunohistochemistry for c-Fos and α-MSH in the hypothalamus. The immunohistochemical methods and the stereotaxic coordinates for the hypothalamic nuclei were based on our previous report (6). Briefly, mice were anesthetized with pentobarbital at 1 h after intracerebroventricular injection of CNP-53 (1.5 nmol/mouse) and perfused with 50 mL 0.1 mol/L PBS, followed by 50 mL ice-cold 4% paraformaldehyde in 0.1 mol/L PBS. Sections of 30-μm thickness were cut with a cryostat. According to the mouse brain atlas (9), cross-sections were selected in correspondence to −1.70 mm [ARC, lateral hypothalamus (LH), dorsomedial hypothalamus (DMH), ventromedial hypothalamic

From the [1]Department of Medicine and Clinical Science, Kyoto University Graduate School of Medicine, Kyoto, Japan; and the [2]Clinical Research Institute, National Hospital Organization, Kyoto Medical Center, Kyoto, Japan.
Corresponding author: Nobuko Yamada-Goto, nobukito@kuhp.kyoto-u.ac.jp.
Received 31 May 2012 and accepted 7 November 2012.
DOI: 10.2337/db12-0718
This article contains Supplementary Data online at http://diabetes.diabetesjournals.org/lookup/suppl/doi:10.2337/db12-0718/-/DC1.

See accompanying commentary, p. 1379.

nucleus (VMH)] and to −0.82 mm [paraventricular nucleus (PVN)], relative to bregma. For c-Fos and α-melanocyte–stimulating hormone (α-MSH) protein staining, the sections were incubated with antic-Fos rabbit antibody (Ab-5; 1:5,000; Oncogene Science, Cambridge, MA) and antiα-MSH sheep antibody (AB5087; 1:10,000; EMD Millipore, Billerica, MA), respectively. The antibody was detected using the Vectastain ABC Elite kit (PK-6101; Vector Laboratories, Burlingame, CA) and a diaminobenzidine substrate kit (SK-4100; Vector Laboratories) was used for visualization. The second antibodies for fluorescence visualization used were goat anti-rabbit488 (A11008; 1:200; Life Technologies, Carlsbad, CA) for antic-Fos rabbit antibody and goat anti-sheep546 (A21098; 1:200; Life Technologies) for antiα-MSH sheep antibody.

Data analysis. All values are given as the mean ± SEM. Statistical analysis of the data were performed by ANOVA, followed by the Tukey-Kramer test. Statistical significance was defined as $P < 0.05$.

RESULTS

Effects of intracerebroventricular administration of CNP-22 and CNP-53 on food intake at refeeding after fasting. The intracerebroventricular administration of CNP-22 (1.5 and 4.5 nmol/mouse) and CNP-53 (1.5 nmol/mouse) significantly suppressed food intake during 4-h refeeding after 48-h fasting in comparison with data from saline-treated mice (Fig. 1*A*). In this experiment, CNP-53 (1.5 nmol), but not other treatments, induced significant reduction of body weight compared with saline treatment (Supplementary Table 2). The mRNA expressions of preopiomelanocortin and cocaine and amphetamine-related peptide significantly decreased, and the mRNA expressions of *NPY* and *AgRP* significantly increased after refeeding compared with control animals (Supplementary Fig. 1). The intracerebroventricular administration of CNP-53 did not influence the mRNA expressions of these neuropeptides in the hypothalamus (Supplementary Fig. 1). Next, the peripheral action of CNP on food intake was examined when a 10-fold greater dose than intracerebroventricular injection of each CNP was intraperitoneally administered. The intraperitoneal administrations of CNP-22 (1.5 μmol/kg) and CNP-53 (0.5 μmol/kg) did not change the food intake during 4-h refeeding after 48-h fasting (Fig. 1*B*), nor were there changes in body weight (Supplementary Table 3).

The intracerebroventricular administrations of CNP-22 (4.5 nmol/mouse) and CNP-53 (1.5 nmol/mouse) at 1 h before the start of the dark phase significantly suppressed nocturnal food intake compared with saline treatment (Fig. 1*C*).

Effect of intracerebroventricular administration of CNP-22 and CNP-53 on NPY-induced and ghrelin-induced food intake. When CNP-22 (4.5 nmol/mouse) and CNP-53 (1.5 nmol/mouse) were concomitantly administered intracerebroventricularly with NPY, they significantly suppressed the food intake induced by NPY compared with that of saline treatment (Fig. 2*A*). When CNP-22 (4.5 nmol/mouse) and CNP-53 (1.5 nmol/mouse) were administered intracerebroventricularly with ghrelin, they significantly suppressed the food intake induced by ghrelin compared with that of saline treatment (Fig. 2*B*).

Effect of melanocortin receptor antagonist, SHU9119, on the anorectic effect of CNP. To examine its involvement in the anorectic effect of CNP, SHU9119 was administered intracerebroventricularly together with CNP-53 (1.5 nmol/mouse). SHU9119 (1 nmol/mouse) significantly attenuated the suppressive action of CNP-53 on the food intake during 4-h refeeding after 48-h fasting, whereas SHU9119 itself significantly enhanced the increase of food intake in comparison with mice administered saline treatment (Fig. 3).

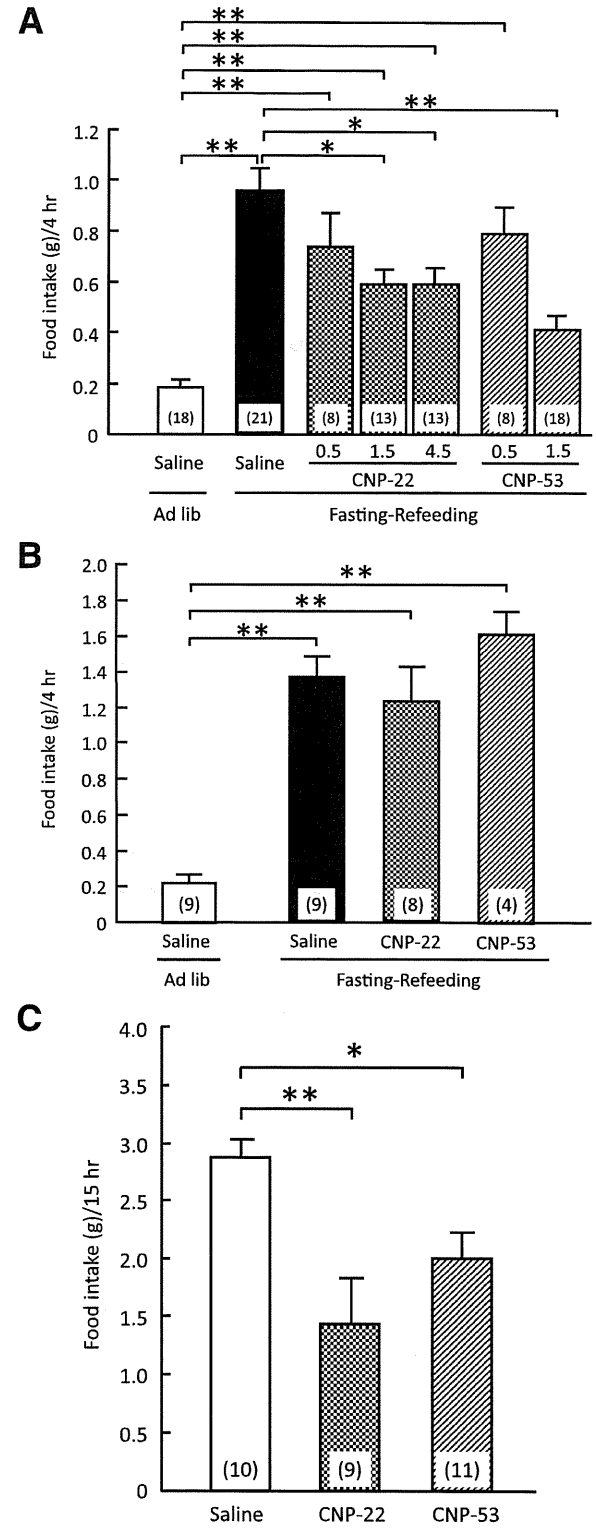

FIG. 1. Effects of CNP on refeeding after fasting. *A*: Effects of intracerebroventricular administration of CNP-22 (0.5, 1.5, and 4.5 nmol/mouse) and CNP-53 (0.5 and 1.5 nmol/mouse) on 4-h refeeding after 48-h fasting in mice. Food intake was observed for 4 h after refeeding. *B*: Effects of intraperitoneal administration of CNP-22 (1.5 μmol/kg) and CNP-53 (0.5 μmol/kg) on 4-h refeeding after 48-h fasting in mice. Food intake was observed for 4 h after refeeding. *C*: Effects of intracerebroventricular administration of CNP-22 (4.5 nmol/mouse) and CNP-53 (1.5 nmol/mouse) on nocturnal food intake in mice. Food intake was observed for 15 h after intracerebroventricular injection. Data represent mean ± SEM. The number of mice is given in parentheses. Significant differences: *$P < 0.05$, **$P < 0.01$.

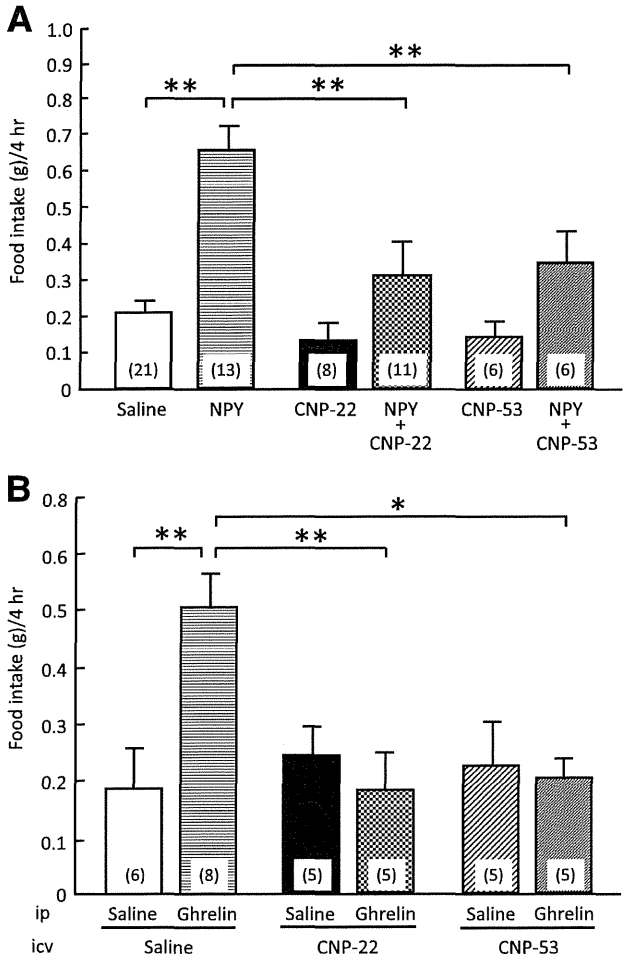

FIG. 2. Effects of CNP-22 and CNP-53 on food intake induced by NPY and ghrelin. *A*: Effects of intracerebroventricular administration of CNP-22 (4.5 nmol/mouse) and CNP-53 (1.5 nmol/mouse) on NPY-induced (5 nmol/mouse, intracerebroventricular) food intake in mice. Food intake was observed for 4 h after coadministration of NPY and CNP. *B*: Effects of intracerebroventricular administration of CNP-22 (4.5 nmol/mouse) and CNP-53 (1.5 nmol/mouse) on ghrelin-induced (100 nmol/kg, intraperitoneal) food intake in mice. Food intake was observed for 4 h after coadministration of ghrelin and CNP. Data represent mean ± SEM. The number of mice is given in parentheses. Significant differences: *$P < 0.05$, **$P < 0.01$.

c-Fos–immunoreactive cells in the hypothalamus after intracerebroventricular administration of CNP. To understand the neuronal pathway involved in the anorectic actions of CNP, the expression of c-Fos, one of the markers of neuronal activation, was monitored by immunohistochemical examination at 1 h after intracerebroventricular injection of CNP-53 (1.5 nmol/mouse). The numbers of c-Fos–immunoreactive cells in the ARC, PVN, and DMH were predominantly increased after intracerebroventricular injection of CNP-53 in comparison with saline treatment (Fig. 4*A*). The c-Fos–positive cells were also moderately increased in the VMH and LH (Fig. 4*A*). Next, we examined whether c-Fos immunoreactivity coexisted with α-MSH–containing cells. In the ARC of saline-treated mice, only a few α-MSH–immunoreactive cells showed weak c-Fos immunoreactivity (Fig. 4*B*). However, c-Fos–immunoreactive cells that increased with intracerebroventricular administration of CNP-53 in the ARC expressed a large amount of α-MSH immunoreactivity (Fig. 4*B*).

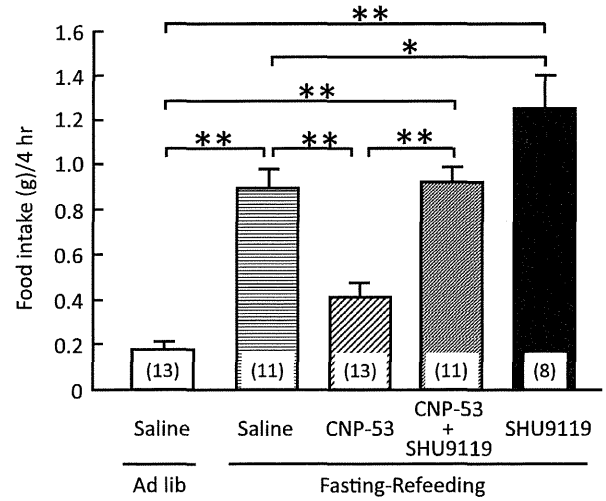

FIG. 3. Effects of intracerebroventricular administration of CNP-53 (1.5 nmol/mouse) and SHU9119 (1 nmol/mouse) on refeeding after 48-h fasting in mice. Food intake was observed for 4 h after refeeding. Data represent mean ± SEM. The number of mice is given in parentheses. Significant differences: *$P < 0.05$, **$P < 0.01$.

DISCUSSION

The current study demonstrated that intracerebroventricular administration of CNP-22 and CNP-53, but not intraperitoneal injection, led to significant reduction of food intake induced by fasting–refeeding. This reduction was inhibited by the melanocortin-3 receptor (MC3R)/melanocortin-4 receptor (MC4R) antagonist SHU9119. In addition, CNP significantly suppressed nocturnal food intake and orexigenic actions induced by NPY and ghrelin. The immunohistochemical study revealed that intracerebroventricular administration of CNP-53 increased the number of c-Fos–expressing cells containing α-MSH in the hypothalamus. These findings indicated that the intracerebroventricular administration of CNP exhibits anorexigenic actions partially via activation of the melanocortin system, although the doses of CNP used in the current study could be pharmacological doses.

The hypothalamus is considered to be an important region in regulating energy homeostasis. In particular, the ARC in the hypothalamus contains both an orexigenic peptide, NPY, and an anorexigenic peptide, α-MSH, and is postulated to be involved in the first-order regulation of food intake. Synthetic MC3R/MC4R agonists, melanotan II, and [Nle^4-D-Phe^7]–α-MSH completely blocked food deprivation–induced increase in food intake as well as the food intake stimulated by intracerebroventricular administration of NPY (10,11). Regarding the reciprocal interactions of α-MSH and NPY, melanocortin neurons in the ARC project to the PVN (12). In the current study, intracerebroventricular administration of CNP significantly suppressed food intake after fasting, which was antagonized by SHU9119. Our results also showed that CNP suppressed NPY-induced food intake. Taken together, these findings indicate that CNP exhibits anorexigenic actions via activation of MC3R/MC4R downstream signaling. However, mRNA expressions of preopiomelanocortin, cocaine and amphetamine-related peptide, *NPY*, and *AgRP* in the hypothalamus after the intracerebroventricular injection of CNP-53 in fasting–refeeding experiment did not change compared with those after saline. The reason for this

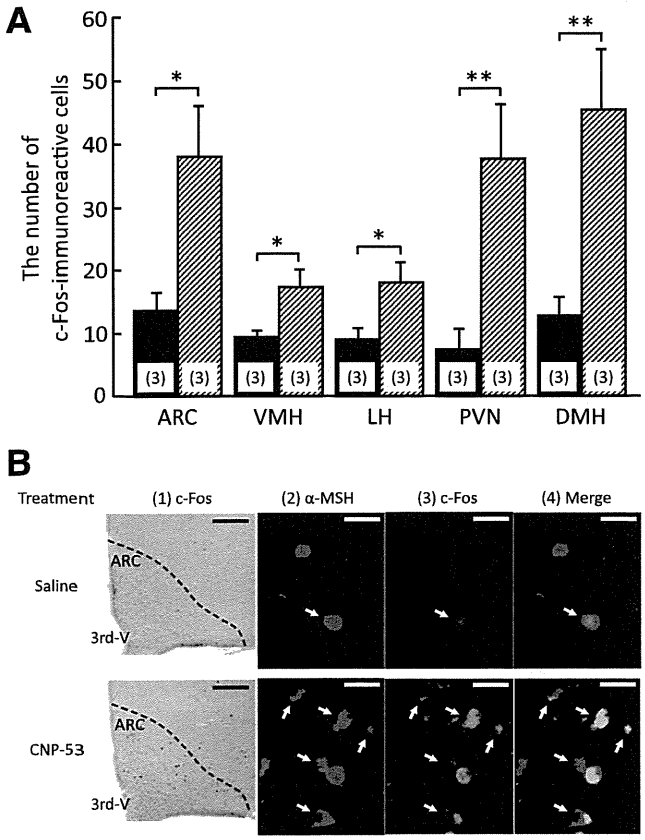

FIG. 4. The c-Fos–immunoreactive cells in the hypothalamus after intracerebroventricular administration of CNP-53 (1.5 nmol/mouse). *A*: Number of c-Fos–immunoreactive cells after saline and CNP-53 treatments. Data represent mean ± SEM. The number of mice is given in parentheses. Significant differences: *$P < 0.05$, **$P < 0.01$. *B*: c-Fos–immunoreactive cells induced by intracerebroventricular administration of saline and CNP-53 (1). 3rd-V, the third ventricular. Scale bars, 100 μm. Coexistence of α-MSH (red) and c-Fos (green) immunoreactivity in the ARC (2–4) after saline (*upper*) and CNP-53 (1.5 nmol/mouse; *lower*) treatments. White arrows indicate cells expressing both α-MSH and c-Fos immunoreactivity. 3rd-V, the third ventricular. Scale bars, 20 μm.

discrepancy may lie in the experimental condition, time course, and regional specificity. To clarify this discrepancy, further examinations will be required.

This study demonstrated that the intracerebroventricular administration of CNP significantly suppressed the nocturnal food intake. Robust feeding during the nocturnal phase of the daily light–dark cycle was demonstrated to be attributed to the upregulation of NPY and its receptors (13). These findings indicate that CNP may decrease food intake in the nocturnal phase via suppression of NPY action.

In the current study, CNP significantly suppressed the increase in food intake induced by ghrelin, an orexigenic hormone secreted by the stomach (14). NPR-B, a CNP receptor, has been identified in appetite-regulating regions, such as the ARC, VMH, PVN, DMH, and LH (15). The systemic administration of ghrelin significantly increased NPY and AgRP expression in the ARC of the hypothalamus in fed and fasted rats (15), resulting in hyperphagia. The intracerebroventricular injection of melanotan II caused a significant decrease in ghrelin-induced food intake (16). These findings suggest that the actions of ghrelin are modulated by α-MSH and NPY systems. Furthermore, plasma ghrelin and hypothalamic ghrelin receptor mRNA expression are reported to be increased after fasting (17,18). These findings suggest the possibility that intracerebroventricular administration of CNP activates the melanocortin system, which subsequently inhibits the action of NPY, resulting in a reduced increase of food intake induced by ghrelin.

To assess which hypothalamic nucleus is involved in the anorexigenic action of CNP, a marker for neuronal activity, c-Fos expression in the hypothalamus was examined after intracerebroventricular administration of CNP-53. The intracerebroventricular administration of CNP-53 significantly increased the number of c-Fos–expressing cells in several hypothalamic nuclei, such as ARC, PVN, DMH, VMH, and LH, indicating that CNP-53 directly or indirectly stimulates neurons in these hypothalamic nuclei. Especially in the ARC, the result was an increased number of c-Fos–immunoreactive cells containing α-MSH immunoreactivity, indicating that CNP stimulates α-MSH–containing neurons. This possibility is supported by the finding that the suppressive action of CNP-53 on food intake was blocked by concomitant administration of SHU9119, an MC3R/MC4R antagonist.

The current study has demonstrated the anorexigenic action of intracerebroventricular administration of CNP via activation of the melanocortin system. To define the precise effect of CNP in the brain on food intake, further investigation using mice with inducible brain-specific deletion of CNP or NPR-B/NPR-C will be required.

From the present findings, we postulate the possible mechanism for anorexigenic action of exogenous CNP to be as follows: CNP directly or indirectly acts on α-MSH–containing neurons and subsequently stimulates α-MSH release, resulting in suppression of food intake induced by NPY and ghrelin. This possible mechanism may apply to the suppressive effects of CNP on food intake after fasting and in the nocturnal phase. Further work is needed to define the pathophysiological significance of brain CNP in regulation of food intake.

ACKNOWLEDGMENTS

This work was supported in part by research grants from the Ministry of Education, Culture, Sports, Science, and Technology of Japan, and the Ministry of Health, Labour, and Welfare of Japan.

No potential conflicts of interest relevant to this article were reported.

N.Y.-G. and G.K. performed experiments, contributed to discussion, and wrote the manuscript. K.E., M.I., Y.O., Y.Y., T.K., A.Y., N.S.-A., H.A., and K.H. contributed to discussion. K.N. contributed to discussion, and reviewed and edited the manuscript. K.N. is the guarantor of this work and, as such, had full access to all the data in the study and takes responsibility for the integrity of the data and the accuracy of the data analysis.

REFERENCES

1. Minamino N, Makino Y, Tateyama H, Kangawa K, Matsuo H. Characterization of immunoreactive human C-type natriuretic peptide in brain and heart. Biochem Biophys Res Commun 1991;179:535–542
2. Herman JP, Langub MC Jr, Watson RE Jr. Localization of C-type natriuretic peptide mRNA in rat hypothalamus. Endocrinology 1993;133:1903–1906
3. Langub MC Jr, Watson RE Jr, Herman JP. Distribution of natriuretic peptide precursor mRNAs in the rat brain. J Comp Neurol 1995;356:183–199
4. Langub MC Jr, Dolgas CM, Watson RE Jr, Herman JP. The C-type natriuretic peptide receptor is the predominant natriuretic peptide receptor mRNA expressed in rat hypothalamus. J Neuroendocrinol 1995;7:305–309

5. Herman JP, Dolgas CM, Rucker D, Langub MC Jr. Localization of natriuretic peptide-activated guanylate cyclase mRNAs in the rat brain. J Comp Neurol 1996;369:165-187
6. Yamada N, Katsuura G, Ochi Y, Ebihara K, Kusakabe T, Hosoda K, Nakao K. Impaired CNS leptin action is implicated in depression associated with obesity. Endocrinology 2011;152:2634–2643
7. Nakao K, Katsuura G, Morii N, Itoh H, Shiono S, Yamada T, Sugawara A, Sakamoto M, Saito Y, Eigyo M, Matsushita A, Imura H. Inhibitory effect of centrally administered atrial natriuretic polypeptide on the brain dopaminergic system in rats. Eur J Pharmacol 1986;131:171–177
8. Yamada N, Katsuura G, Tatsuno I, et al. Orexin decreases mRNA expressions of NMDA and AMPA receptor subunits in rat primary neuron cultures. Peptides 2008;29:1582–1587
9. Paxinos G, Franklin KBJ. *The mouse brain in stereotaxic coordinates.* New York, Academic Press, 2004
10. Brown KS, Gentry RM, Rowland NE. Central injection in rats of alpha-melanocyte-stimulating hormone analog: effects on food intake and brain Fos. Regul Pept 1998;78:89–94
11. Murphy B, Nunes CN, Ronan JJ, et al. Melanocortin mediated inhibition of feeding behavior in rats. Neuropeptides 1998;32:491–497
12. Sánchez E, Singru PS, Acharya R, et al. Differential effects of refeeding on melanocortin-responsive neurons in the hypothalamic paraventricular nucleus. Endocrinology 2008;149:4329–4335
13. Kalra PS, Dube MG, Xu B, Farmerie WG, Kalra SP. Evidence that dark-phase hyperphagia induced by neurotoxin 6-hydroxydopamine may be due to decreased leptin and increased neuropeptide Y signaling. Physiol Behav 1998;63:829–835
14. Kojima M, Hosoda H, Date Y, Nakazato M, Matsuo H, Kangawa K. Ghrelin is a growth-hormone-releasing acylated peptide from stomach. Nature 1999;402:656–660
15. Harrold JA, Dovey T, Cai XJ, Halford JC, Pinkney J. Autoradiographic analysis of ghrelin receptors in the rat hypothalamus. Brain Res 2008;1196:59–64
16. Shrestha YB, Wickwire K, Giraudo SQ. Action of MT-II on ghrelin-induced feeding in the paraventricular nucleus of the hypothalamus. Neuroreport 2004;15:1365–1367
17. Keen-Rhinehart E, Bartness TJ. NPY Y1 receptor is involved in ghrelin- and fasting-induced increases in foraging, food hoarding, and food intake. Am J Physiol Regul Integr Comp Physiol 2007;292:R1728–R1737
18. Kim MS, Yoon CY, Park KH, et al. Changes in ghrelin and ghrelin receptor expression according to feeding status. Neuroreport 2003;14:1317–1320

THE JOURNAL OF BIOLOGICAL CHEMISTRY VOL. 287, NO. 48, pp. 40441–40447, November 23, 2012

Leptin Activates Hepatic 5′-AMP-activated Protein Kinase through Sympathetic Nervous System and α1-Adrenergic Receptor

*A POTENTIAL MECHANISM FOR IMPROVEMENT OF FATTY LIVER IN LIPODYSTROPHY BY LEPTIN**

Received for publication, June 16, 2012, and in revised form, September 24, 2012 Published, JBC Papers in Press, September 28, 2012, DOI 10.1074/jbc.M112.384545

Licht Miyamoto[‡1], Ken Ebihara[‡§2], Toru Kusakabe[‡], Daisuke Aotani[‡], Sachiko Yamamoto-Kataoka[‡], Takeru Sakai[‡], Megumi Aizawa-Abe[‡§], Yuji Yamamoto[‡], Junji Fujikura[‡], Tatsuya Hayashi[¶], Kiminori Hosoda[‡§‖], and Kazuwa Nakao[‡§]

From the [‡]Department of Medicine and Clinical Science, Kyoto University Graduate School of Medicine and the [§]Translational Research Center, Kyoto University Hospital, 54 Shogoin Kawahara-cho, Sakyo-ku, Kyoto 606-8507, the [¶]Kyoto University Graduate School of Human and Environmental Studies, Yoshida-Nihonmatsu-cho, Sakyo-ku, Kyoto 606-8501, and the [‖]Department of Human Health Science, Kyoto University Graduate School of Medicine, 54 Shogoin Kawahara-cho, Sakyo-ku, Kyoto 606-8507, Japan

Background: AMPK activation promotes glucose and lipid metabolism.
Results: Hepatic AMPK activities were decreased in fatty liver from lipodystrophic mice, and leptin activated the hepatic AMPK via the α-adrenergic effect.
Conclusion: Leptin improved the fatty liver possibly by activating hepatic AMPK through the central and sympathetic nervous systems.
Significance: Hepatic AMPK plays significant roles in the pathophysiology of lipodystrophy and metabolic action of leptin.

Leptin is an adipocyte-derived hormone that regulates energy homeostasis. Leptin treatment strikingly ameliorates metabolic disorders of lipodystrophy, which exhibits ectopic fat accumulation and severe insulin-resistant diabetes due to a paucity of adipose tissue. Although leptin is shown to activate 5′-AMP-activated protein kinase (AMPK) in the skeletal muscle, the effect of leptin in the liver is still unclear. We investigated the effect of leptin on hepatic AMPK and its pathophysiological relevance in A-ZIP/F-1 mice, a model of generalized lipodystrophy. Here, we demonstrated that leptin activates hepatic AMPK through the central nervous system and α-adrenergic sympathetic nerves. AMPK activities were decreased in the fatty liver of A-ZIP/F-1 mice, and leptin administration increased AMPK activities in the liver as well as in skeletal muscle with significant reduction in triglyceride content. Activation of hepatic AMPK with A769662 also led to a decrease in hepatic triglyceride content and blood glucose levels in A-ZIP/F-1 mice. These results indicate that the down-regulation of hepatic AMPK activities plays a pathophysiological role in the metabolic disturbances of lipodystrophy, and the hepatic AMPK activation is involved in the therapeutic effects of leptin.

Leptin is an adipocyte-derived hormone that regulates energy homeostasis mainly through the hypothalamus (1, 2). In addition to food intake and energy expenditure, leptin regulates glucose and lipid metabolism. Indeed, the usefulness of leptin treatment in various types of diabetes, including type 1, type 2, and lipoatrophic diabetes, has been demonstrated in rodent models (3–8). The clinical application of leptin treatment has already begun (9–12), especially in lipoatrophic diabetes that develops with lipodystrophy.

Lipodystrophy is a disease characterized by a paucity of adipose tissue that leads to leptin deficiency. Patients with lipodystrophy generally suffer severe insulin-resistant diabetes. Although the molecular mechanism by which insulin resistance develops in lipodystrophy is not fully understood, ectopic fat accumulation in insulin target tissues such as skeletal muscle and liver is thought to be one of the major causes for insulin resistance. The pathological condition in which ectopically accumulated fat exerts adverse effects against the cellular function is referred to as "lipotoxicity" (13). The amount of fat accumulated in tissues is known to correlate with the severity of insulin resistance (14). Lipoatrophic patients frequently develop severe fatty liver and excess fat accumulation in the skeletal muscle (15).

We and others have demonstrated that leptin effectively improves insulin sensitivity accompanied by dramatic reduction of fat content in the liver and skeletal muscle in patients

* This work was supported in part by research grants from the Ministry of Education, Culture, Sports, Science and Technology of Japan, the Ministry of Health, Labor and Welfare of Japan, The Takeda Medical Research Foundation, The Japan Foundation of Applied Enzymology, Eli Lilly and Co., and The Nakatomi Foundation.
[1] Present address: Dept. of Medical Pharmacology, Institute of Health Biosciences, University of Tokushima Graduate School, 1-78-1 Shou-machi, Tokushima-shi, Tokushima 770-8505, Japan.
[2] To whom correspondence should be addressed: 54 Shogoin Kawahara-cho, Sakyo-ku, Kyoto 606-8507, Japan. Tel.: 81-757513173; Fax: 81-757719452; E-mail: kebihara@kuhp.kyoto-u.ac.jp.

with lipodystrophy (3, 9–12). Using rodent models, it was demonstrated that leptin activates AMPK[3] in the skeletal muscle through both central and direct pathways (16). AMPK is a heterotrimeric enzyme that is conserved from yeast to humans and functions as a "fuel gauge" to monitor the status of cellular energy. AMPK potently stimulates fatty acid oxidation by inhibiting the activity of acetyl-CoA carboxylase (17). Thus, AMPK activation by leptin is a plausible mechanism by which leptin reduces ectopic fat in the skeletal muscle.

In addition to the skeletal muscle, recent studies have shown the physiological significance of AMPK in the liver (18–20). However, the effect of leptin on hepatic AMPK activity remains to be determined. The role of AMPK in the pathogenesis of metabolic abnormalities in lipodystrophy also remains unclear. In this study, we investigated the effect of leptin on hepatic AMPK activities and the pathophysiological role of AMPK in A-ZIP/F-1 mice, a well established mouse model of generalized lipodystrophy (21).

EXPERIMENTAL PROCEDURES

Materials and Animals—All reagents were analytic grade and obtained from Sigma unless otherwise stated. C57BL/6J mice and Wistar rats were purchased from Japan SLC, Inc. The F1 mice analyzed in Fig. 4 were obtained by crossing male A-ZIP/F-1 mice on the FVB/N background with female leptin transgenic mice on the C57BL/6J background (3, 22). A-ZIP/F-1 and the F1 mice were studied with appropriate littermate controls. Mice and rats were housed in an animal facility maintained at 20 °C with a 12:12-h light/dark cycle, allowed free access to water and standard rodent chow, and were randomly assigned to experimental groups. The mice were analyzed at the age of 9–10 weeks (C57BL/6J) or 15 weeks (A-ZIP/F-1, F1). Kyoto University Graduate School of Medicine Committee on Animal Research approved all experimental procedures.

Drug Administration—For continuous treatment, leptin was administered for 6 days using a subcutaneously implanted osmotic pump (Durect) at the dose of 0.65 mg/kg/day. For single intraperitoneal and intracerebroventricular (i.c.v.) injection, the dose of leptin was 1 mg/kg and 1 μg/mouse, respectively. Prazosin (2.5 mg/kg/day) or propranolol (1 mg/kg/day) was continuously co-administered with leptin for 6 days using an independently implanted osmotic pump. A769662 was administered once daily by intraperitoneal injection at the dose of 30 mg/kg/day for 4 days.

Primary Hepatocyte—Hepatocytes were isolated from male Wistar rats (100–150 g) by a two-step collagenase perfusion. The portal vein was cannulated under chloral hydrate anesthesia, and the liver was perfused with hepatocyte liver perfusion medium and digest medium (Invitrogen). After perfusion, hepatocytes were purified by filtration (100-μm mesh) and centrifuged (100 × *g*, 1 min, four times) and seeded onto 6-well culture plates coated with type I collagen (Iwaki) (1×10^6 cells/well). Cells were cultured in DMEM containing 10% FBS, 100 nM insulin, 100 nM dexamethasone, 30 mg/liter kanamycin, and 5 units/ml aprotinin for 12 h, and the medium were replaced with DMEM containing 10% FBS, 1 nM insulin, 1 nM dexamethasone, 30 mg/liter kanamycin, and 5 units/ml aprotinin for 6 h prior to stimulation. The cells were stimulated by 100 ng/ml leptin, 1 mM 5-aminoimidazole-4-carboxamide 1-β-D-ribofuranoside or 0.5 mM 2,4-dinitrophenol for the indicated times.

Hepatic Vagotomy—Hepatic vagotomy was performed as described previously (23, 24) with modifications. Briefly, a hepatic branch of the ventral subdiaphragmatic vagal trunk was cleft using micro scissors under ether anesthesia, and the abdominal muscle wall and skin incision was closed with silk sutures. Drugs were introduced 1 week after the surgery. Accomplishment of the amputation was visually confirmed when sampling.

Chemical Sympathectomy—C57BL/6J mice were chemically sympathectomized by continuous infusion of guanethidine (30 mg/kg/day) for 6 days as described above.

Tissue Sampling and Biochemical Analysis—Tissues were rapidly isolated and frozen in liquid nitrogen by freeze-clamping (25) under chloral hydrate anesthesia after starvation for 6 h. Mice had been starved for 4 h previous to and during the study in a single administration study. Blood glucose was determined by reflectance glucometer under *ad libitum* feeding conditions. Plasma leptin was measured by RIA (Linco). Plasma insulin (Morinaga), adiponectin (Linco), and interleukin-6 (R&D Systems) were measured by ELISA. Triglyceride content was determined by E-test kit (Wako) in 2-propanol/heptane extract of the tissues. Homeostasis model assessment insulin resistance (HOMA-IR) was calculated on the assumption that the titer of murine insulin is as much as that of human insulin.

Isoform-specific AMPK Activity—AMPK activities were determined as described previously (26). Briefly, frozen tissues were homogenized in Hepes/Triton-based lysis buffer and then centrifuged. The supernatants were immunoprecipitated with protein A-Sepharose beads and isoform-specific antibodies against AMPK α1 or α2 (Millipore). Kinase activities in the immune complex were determined by the phosphorylation of the SAMS peptide using [γ-^{32}P]ATP.

Western Blotting Analysis—40 μg of protein per each sample was subjected to SDS-PAGE using 4–12% BisTris gel (Bio-Rad). Antibodies were from Cell Signaling Technology or Merck. ECL Plus (GE Healthcare) and LAS-1000 image analyzer (Fuji film) were used for detection and quantification.

Quantitative Analysis of Gene Expressions—Total RNA was prepared using Isogen (Molecular Research Center). mRNA levels were quantified by real time PCR with the Taqman method (ABI Prism 7300). Primer sets and probes were as follows: 18 S, CGCGCAAATTACCCACTCCCGA, CGGCTACCACATCCAAGGA, and CCAATTACAGGGCCTCGAAA; AMPKα1, TGCAAAGATAGCCGACTTTGGTCTTTCA, GAACGTCCTGCTTGATGCACACAT, and TGGGTGAGCCACAGCTTGTTCTTA; and AMPKα2, TGATTCCAGCACAGCTGAGAACCACT, AAGCATCGATGATGAGGTGGTGGA, and ACAAAGTGCTGCCAGTCAAAGAGC (probe, forward, and reverse, respectively) Relative amounts of mRNAs were normalized with the ribosomal 18 S RNA.

[3] The abbreviations used are: AMPK, 5′-AMP-activated protein kinase; A-ZIP, A-ZIP/F-1 mice; LepTg, transgenic mice overexpressing leptin; BisTris, 2-[bis(2-hydroxyethyl)amino]-2-(hydroxymethyl)propane-1,3-diol; HOMA-IR, homeostasis model assessment insulin resistance; i.c.v., intracerebroventricular.

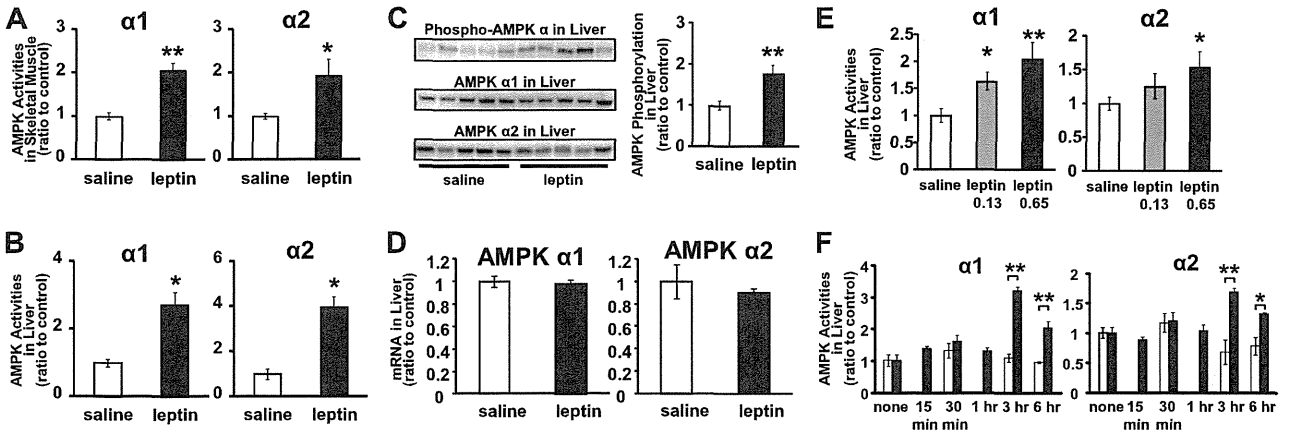

FIGURE 1. **AMPK activation in skeletal muscle and liver by leptin administration.** Isoform-specific AMPK activities in gastrocnemius muscle (*A*) and liver (*B*) from C57BL/6J mice after continuous saline or leptin administration are shown. Western blot analyses for phospho-AMPKα, AMPK α1 and α2 (*C*), and AMPK α1 and α2 mRNA levels normalized to 18 S ribosomal RNA (*D*) in liver are shown. AMPK activities in liver after 0.13 and 0.65 mg/kg/day continuous leptin infusion (*E*) are shown. AMPK activities in liver 15 min to 6 h after single intraperitoneal injection of saline or leptin (*F*) are shown. Data are shown as ratios to saline or quiescent control (mean ± S.E.). □, saline; ■, leptin. $n = 4-6$. *, $p < 0.05$; **, $p < 0.01$ *versus* saline.

Statistical Analyses—Two groups were compared by Student's *t* test. Comparisons between multiple groups were evaluated by analysis of variance. $p < 0.05$ was considered statistically significant.

RESULTS

Effect of Leptin Treatment on AMPK α1 and α2 Activities in Skeletal Muscle and Liver—The isoform-specific AMPK activities in skeletal muscles and liver were determined in leptin- and saline-treated mice. Both AMPK α1 and α2 activities in skeletal muscle were increased 2-fold in leptin-treated mice compared with saline-treated mice (Fig. 1*A*). AMPK α1 and α2 activities in the liver were also increased 2.5- and 3.5-fold, respectively (Fig. 1*B*). The phosphorylation of AMPK α was also increased in leptin-treated mice compared with saline-treated mice (Fig. 1*C*). Meanwhile, protein or mRNA expressions of AMPK α1 and α2 in the liver were not significantly different between leptin- and saline-treated mice (Fig. 1, *C* and *D*). Therefore, the increase of AMPK activities in the liver from leptin-treated mice was not due to the increase in their expression levels.

When leptin was administered continuously, the activation of AMPK in the liver was dose-dependent (Fig. 1*E*). After intraperitoneal single leptin injection, the activation of both AMPK α1 and α2 was detected from 3 h while no activation was observed within 1 h (Fig. 1*F*).

Mechanism of Hepatic AMPK Activation by Leptin—To clarify whether leptin acts directly on hepatocytes, we examined AMPK activities in isolated primary rat hepatocytes with or without leptin (Fig. 2*A*). The addition of leptin into the culture medium increased neither AMPK α1 nor α2 activities. Next, we examined the effect of leptin i.c.v. injection on AMPK activities in the liver (Fig. 2*B*). The activation of both AMPK α1 and α2 was detected 3 h after leptin injection at the dose that did not cause any effect when administered peripherally. These results indicate that leptin activates AMPK in the liver mainly through the CNS.

Therefore, we examined the involvement of autonomic nerves in the effect of leptin on AMPK activation in the liver. Hepatic vagotomy did not show any effect on AMPK activation by leptin in the liver (Fig. 2*C*). In contrast, chemical sympathectomy by guanethidine treatment completely inhibited the activation of both AMPK α1 and α2 by leptin in the liver (Fig. 2*D*). We further investigated the involvement of the subtype-specific sympathetic nervous system. Administration of propranolol, a β-antagonist, did not suppress AMPK activation in the liver, whereas prazosin, an α1-antagonist, completely inhibited the activation of both AMPK α1 and α2 by leptin in the liver (Fig. 2, *E* and *F*).

AMPK α1 and α2 Activities in Skeletal Muscle and Liver from A-ZIP/F-1 Mice—To explore the pathophysiological role of AMPK in lipodystrophy, we examined AMPK α1 and α2 activities in skeletal muscle and liver from A-ZIP/F-1 (A-ZIP) mice. Characteristics of A-ZIP mice used in this study are shown in Table 1. Consistent with previous studies (21), A-ZIP mice showed hyperglycemia and hyperinsulinemia, suggesting insulin resistance, and also showed increased liver weight, suggesting fatty liver. Plasma leptin and adiponectin levels were markedly decreased, but the plasma interleukin-6 level was not significantly different from that in WT mice. In these A-ZIP mice, both AMPK α1 and α2 activities in the liver were apparently decreased compared with WT mice, although those in the skeletal muscle were not significantly different from WT mice (Fig. 3, *A* and *B*). AMPK α1 and α2 mRNA expressions in the skeletal muscle were not significantly different in A-ZIP mice, and those in the liver were rather increased compared with WT mice (Fig. 3, *C* and *D*). Therefore, the decrease in AMPK activities in the liver from A-ZIP mice was not due to the change in their mRNA expressions. However, leptin treatment effectively increased AMPK α1 and α2 activities in the liver as well as in the skeletal muscle from A-ZIP mice (Fig. 3, *E* and *F*).

Effect of Transgenic Overexpression of Leptin on AMPK α1 and α2 Activities in Skeletal Muscle and Liver from A-ZIP/F-1 Mice—To explore the chronic effect of leptin, we crossed transgenic mice overexpressing leptin (LepTg) and A-ZIP mice, producing mice of four genotypes as follows: WT, LepTg, A-ZIP, and A-ZIP/LepTg. AMPK α1 and α2 activities in both the skel-

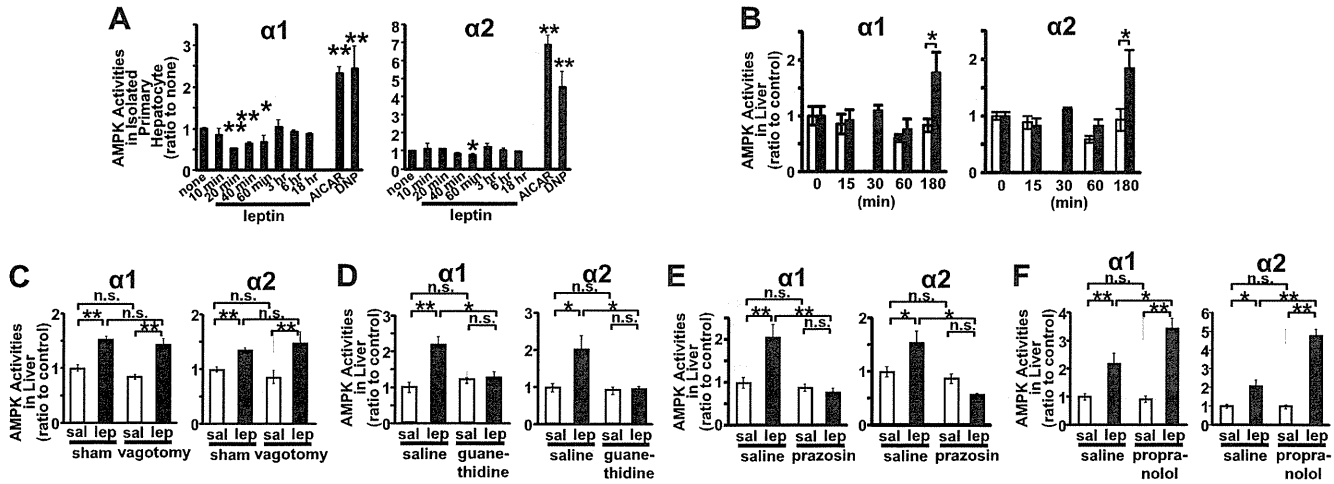

FIGURE 2. **Mechanism of hepatic AMPK activation by leptin administration.** AMPK activities in isolated rat primary hepatocytes 10 min to 18 h after stimulation by leptin, 5-aminoimidazole-4-carboxamide 1-β-D-ribofuranoside (*AICAR*) (40 min), or 2,4-dinitrophenol (*DNP*) (15 min) (*A*) are shown. AMPK activities in liver 15 min to 3 h after i.c.v. administration of saline (*sal*) or leptin (*lep*) (*B*). The effects of hepatic vagotomy (*C*), chemical sympathectomy (*D*), co-administration of antagonists against α1-adrenoreceptors (*E*) or β-adrenoreceptors (*F*) on hepatic AMPK activation by leptin are shown. Data are shown as ratios to saline or quiescent control (mean ± S.E.). $n = 4-6$ (*A*, and *C–E*); $n = 3-6$ (*B*). *, $p < 0.05$; **, $p < 0.01$ *versus* control. *n.s.*, not significant.

TABLE 1

Characteristics of A-ZIP/F-1 mice used in this study

Values are as follows: $n = 8-11$ (glucose); $n = 3-5$ (leptin); $n = 5-7$ (other adipocytokines).

	WT	A-ZIP/F-1 mice
Body weight	30.7 ± 0.8 g	32.5 ± 0.4 g
Glucose	167 ± 5.8 mg/dl	331 ± 39 mg/dl[a]
Insulin	0.24 ± 0.0 ng/ml	0.46 ± 0.1 ng/ml[b]
Leptin	6.15 ± 1.3 ng/ml	1.25 ± 0.5 ng/ml[b]
Adiponectin	6.27 ± 0.4 μg/ml	1.46 ± 0.5 μg/ml[a]
Interleukin-6	5.3 ± 0.8 pg/ml	6.5 ± 1.0 pg/ml
Liver weight	1.19 ± 0.0 g	1.98 ± 0.2 g[a]

[a] $p < 0.01$ *versus* WT. Data are expressed as means ±S.E.
[b] $p < 0.05$ *versus* WT. Data are expressed as means ±S.E.

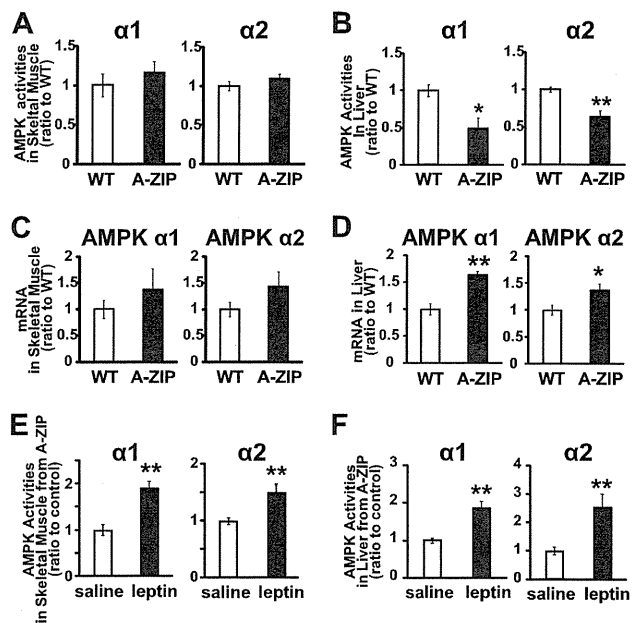

FIGURE 3. **AMPK activities and mRNA expressions in a mouse model of lipoatrophic diabetes.** α1- and α2-isoform-specific AMPK activities in the soleus muscle (*A*) and liver (*B*) are shown. AMPK α1 and α2 mRNA levels in the soleus muscle (*C*) and liver (*D*) normalized to 18 S ribosomal RNA are shown. AMPK activities in gastrocnemius muscle (*E*) and liver (*F*) from A-ZIP/F-1 mice after continuous leptin administration are shown. Data are shown as ratios to WT or saline control (mean ± S.E.). □, WT; ■, A-ZIP/F-1. $n = 4-5$. (*A–D*). □, saline; ■, leptin. $n = 9-10$ (*E* and *F*). *, $p < 0.05$; **, $p < 0.01$ *versus* control.

etal muscle and liver were markedly increased in LepTg mice (Fig. 4, *A* and *B*). At this time, triglyceride contents in skeletal muscle and liver in LepTg mice were reduced to more than half of those in WT mice (Fig. 4, *C* and *D*). AMPK activities were unchanged in the skeletal muscle but were apparently decreased in the liver from A-ZIP mice when compared with WT mice (Fig. 4, *A* and *B*). As to triglyceride contents, the apparent increment was observed in both the skeletal muscle and liver in A-ZIP mice (Fig. 4, *C* and *D*). However, AMPK activities were increased, and triglyceride content was decreased in A-ZIP/LepTg mice as well as in LepTg mice in both the skeletal muscle and liver (Fig. 4, *A–D*). In accordance with our previous report, blood glucose and plasma insulin levels were lower in LepTg mice than in WT mice, and severe hyperglycemia and hyperinsulinemia in A-ZIP mice were strikingly ameliorated by transgenic overexpression of leptin (Fig. 4, *E* and *F*) (3).

Effect of AMPK Activator, A769662, on AMPK Activities and Triglyceride Content in Skeletal Muscle and Liver from A-ZIP/F-1 Mice—After intraperitoneal single injection of A769662, an AMPK-specific activator, the activity of AMPK α1 was increased but that of α2 was not significantly increased in the skeletal muscle (Fig. 5*A*). The activity of both AMPK α1 and α2 was clearly increased in the liver (Fig. 5*B*). Although repetitive injection of A769662 for 4 days did not significantly reduce triglyceride content in the skeletal muscle, it effectively reduced triglyceride content to one-third of that in saline-treated mice in the liver (Fig. 5, *C* and *D*). At this time, the blood glucose level was significantly decreased, and HOMA-IR, an index of insulin resistance, tended to be decreased although plasma insulin level was not significantly decreased (Fig. 5, *E–G*). Food intake and body weight were not affected by A769662 (Fig. 5, *H* and *I*).

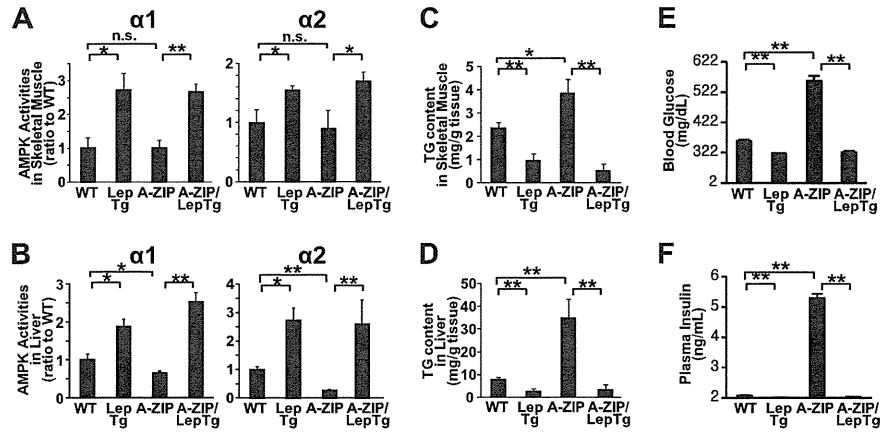

FIGURE 4. **AMPK activation and reduction in ectopic triglyceride accumulation in skeletal muscle and liver from leptin transgenic mice and double transgenic A-ZIP/LepTg mice.** AMPK activities in gastrocnemius muscle (*A*) and liver (*B*), triglyceride content in gastrocnemius muscle (*C*) and liver (*D*), and blood glucose levels (*E*) and plasma insulin levels (*F*) from F1 mice obtained by crossing A-ZIP/F-1 mice and leptin transgenic mice are shown. Data are shown as ratios to +/+ (mean ± S.E.). $n = 4–7$. *, $p < 0.05$; **, $p < 0.01$; *n.s.*, not significant.

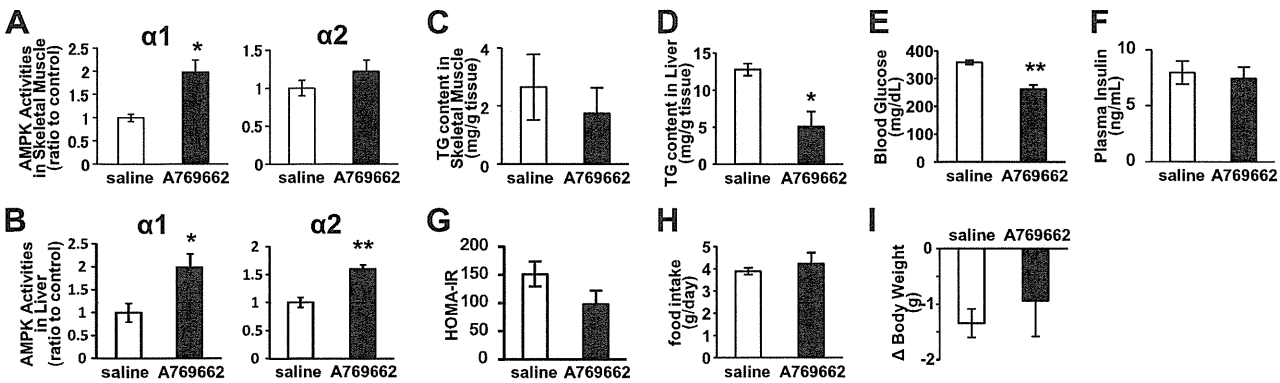

FIGURE 5. **Resolution of fatty liver in A-ZIP/F-1 mice by AMPK activation.** AMPK activities in gastrocnemius muscle (*A*) and liver (*B*) 30 min after a single intraperitoneal injection of AMPK activator, A769662 (30 mg/kg) are shown. Triglyceride contents in gastrocnemius muscle (*C*) and liver (*D*), blood glucose (*E*), plasma insulin (*F*), and calculated HOMA-IR (*G*) after the repetitive A769662 administration (30 mg/kg/day for 4 days) are shown. Food intake (*H*) and weight change (*I*) during the study period are shown.

DISCUSSION

This is the first report clearly demonstrating that leptin activates hepatic AMPK through the central nervous system and an α-adrenergic effect *in vivo*. It had long been unclear whether leptin activates hepatic AMPK *in vivo*. It was reported that adenovirus-induced leptin overexpression failed to increase hepatic AMPK activities (27). However, leptin-induced suppression of gluconeogenesis was abolished in liver-specific AMPK α2 knock-out mice, suggesting that leptin suppresses gluconeogenesis through hepatic AMPK activation (18). Furthermore, a slight increase in hepatic AMPK activity 45 min after leptin administration was reported in mice, although it has been deemed as an artificial effect (28, 29). In this study, we demonstrated that hepatic AMPK activation by leptin is dose-dependent (Fig. 1*E*), and hepatic AMPK activity clearly increases from 3 h after leptin administration in mice (Fig. 1*F*).

In the skeletal muscle, AMPK is reported to be activated by leptin both directly on skeletal muscles and indirectly through the hypothalamic relay (16). In the liver, this study demonstrated that leptin activates AMPK mainly through the CNS and that leptin has no direct AMPK-activating effect on hepatocytes (Fig. 2, *A* and *B*). There is a report showing the increase in AMPK phosphorylation by leptin using Huh7 human hepatoma cells overexpressing leptin receptors; however, it was observed only in the receptor-overexpressing cells (30). AMPK activation in the skeletal muscle by leptin is biphasic, and the former phase, which occurred in 15 min, is caused by direct muscle stimulation (16). Meanwhile, hepatic AMPK activation was detected only from 3 h after leptin administration, supporting the notion that leptin activates hepatic AMPK mainly through the CNS.

The parasympathetic and sympathetic nervous systems between the hypothalamus and liver play an important role in regulating metabolism (31). In this study, chemical sympathectomy completely inhibited hepatic AMPK activation by leptin although hepatic vagotomy did not, indicating that leptin activates hepatic AMPK mainly through the sympathetic nervous system (Fig. 2, *C* and *D*). Moreover, we demonstrated that hepatic AMPK activation by leptin was mainly dependent on the α-adrenergic effect but not on the β-adrenergic effect (Fig. 2, *E* and *F*). Not the β- but the α1-adrenoreceptor stimulation was shown to activate AMPK in isolated skeletal muscle, L6 myotubes, H9C2 cardiomyocyte, and rat heart (16, 32, 33), although not the α1- but the β-adrenoreceptors mediate AMPK activation in brown and white adipocytes (32, 34). The

physiological significance of this adrenoreceptor tissue specificity will be an issue in the future.

Recent reports have revealed some adipocytokines harbor the potential to activate AMPK in the liver or skeletal muscle. AMPK potently stimulates fatty acid oxidation by inhibiting the activity of acetyl-CoA carboxylase (17). Thus, we hypothesized that AMPK might play a pathophysiological role in ectopic fat accumulation and marked insulin resistance developed in lipodystrophy. Indeed, analysis of A-ZIP mice revealed the decrease in AMPK activities in the liver, suggesting the pathophysiological significance of hepatic AMPK in the development of fatty liver in lipodystrophy (Fig. 3*B*).

It is interesting that AMPK activities in the skeletal muscle were not decreased in A-ZIP mice when compared with WT mice. Basal AMPK activities in the skeletal muscle in *fa/fa* rats were also not different from those from control rats (35, 36), although AMPK activities in the liver in *fa/fa* rats and *ob/ob* mice were decreased (37). Although it is unknown what determines the difference between the skeletal muscle and the liver, some factors may counteract the decrease of AMPK activities brought by leptin deficiency in the skeletal muscle.

We previously showed that transgenic overexpression of leptin strikingly improves metabolic abnormalities in A-ZIP mice (3). Insulin-stimulated PI3K activity in the skeletal muscle and liver were amplified in LepTg mice (22). However, the underlying molecular mechanisms of metabolic action of leptin have not been fully clarified. Although leptin was reported to activate AMPK in the skeletal muscle (16), the effect of leptin on hepatic AMPK activity had been unclear. We found that leptin activates both isoforms of AMPK not only in the skeletal muscle but also in the liver in association with the reduction of tissue triglyceride content in A-ZIP mice (Fig. 4). These results indicated the therapeutic role of AMPK in the metabolic improvement by leptin in lipodystrophy.

To confirm the therapeutic role of hepatic AMPK in the improvement of fatty liver by leptin in lipodystrophy, we investigated the effect of A769662, an AMPK-specific activator on liver triglyceride content in A-ZIP mice. A769662 was shown to activate AMPK and decrease acetyl-CoA carboxylase activity and triglyceride in the liver of *ob/ob* mice (38). It was also reported that A769662 preferably works on the liver *in vivo* due to the preference of tissue distribution of A769662 after injection (38). Indeed, although A769662 significantly activated only AMPK α1 and did not significantly decrease triglyceride content in the skeletal muscle, it effectively activated both AMPK α1 and α2 and reduced triglyceride content to one-third in the liver from A-ZIP mice (Fig. 5, *A–D*). These results indicated that hepatic AMPK activation is involved in the improvement of fatty liver by leptin in lipodystrophy. We could not find obvious decrease in the insulin levels. but the HOMA-IR tended to decrease, suggesting hepatic AMPK activation leads to improvement of insulin resistance in lipodystrophy (Fig. 5, *F* and *G*).

In conclusion, this study demonstrates that leptin activates AMPK not only in the skeletal muscle but also in the liver in mice. Leptin activates hepatic AMPK mainly through the CNS and α-adrenergic effects of sympathetic nerves. This study also indicates that hepatic AMPK is involved in the development of metabolic disorders and their improvement by leptin in A-ZIP mice. This study provides the useful notion to understand the molecular mechanism by which leptin regulates energy metabolism and will guide the development of novel metabolic pharmaceuticals.

Acknowledgments—We thank Yoko Koyama and Mayumi Nagamoto for secretarial and technical assistance and Drs. Shuichi Koda, Hideki Matsumoto, and Fumihiko Yokoya for helpful technical advice.

REFERENCES

1. Halaas, J. L., Boozer, C., Blair-West, J., Fidahusein, N., Denton, D. A., and Friedman, J. M. (1997) Physiological response to long term peripheral and central leptin infusion in lean and obese mice. *Proc. Natl. Acad. Sci. U.S.A.* **94,** 8878–8883
2. Campfield, L. A., Smith, F. J., Guisez, Y., Devos, R., and Burn, P. (1995) Recombinant mouse OB protein. Evidence for a peripheral signal linking adiposity and central neural networks. *Science* **269,** 546–549
3. Ebihara, K., Ogawa, Y., Masuzaki, H., Shintani, M., Miyanaga, F., Aizawa-Abe, M., Hayashi, T., Hosoda, K., Inoue, G., Yoshimasa, Y., Gavrilova, O., Reitman, M. L., and Nakao, K. (2001) Transgenic overexpression of leptin rescues insulin resistance and diabetes in a mouse model of lipoatrophic diabetes. *Diabetes* **50,** 1440–1448
4. Miyanaga, F., Ogawa, Y., Ebihara, K., Hidaka, S., Tanaka, T., Hayashi, S., Masuzaki, H., and Nakao, K. (2003) Leptin as an adjunct of insulin therapy in insulin-deficient diabetes. *Diabetologia* **46,** 1329–1337
5. Naito, M., Fujikura, J., Ebihara, K., Miyanaga, F., Yokoi, H., Kusakabe, T., Yamamoto, Y., Son, C., Mukoyama, M., Hosoda, K., and Nakao, K. (2011) Therapeutic impact of leptin on diabetes, diabetic complications, and longevity in insulin-deficient diabetic mice. *Diabetes* **60,** 2265–2273
6. Wang, M. Y., Chen, L., Clark, G. O., Lee, Y., Stevens, R. D., Ilkayeva, O. R., Wenner, B. R., Bain, J. R., Charron, M. J., Newgard, C. B., and Unger, R. H. (2010) Leptin therapy in insulin-deficient type I diabetes. *Proc. Natl. Acad. Sci. U.S.A.* **107,** 4813–4819
7. Shimomura, I., Hammer, R. E., Ikemoto, S., Brown, M. S., and Goldstein, J. L. (1999) Leptin reverses insulin resistance and diabetes mellitus in mice with congenital lipodystrophy. *Nature* **401,** 73–76
8. Kusakabe, T., Tanioka, H., Ebihara, K., Hirata, M., Miyamoto, L., Miyanaga, F., Hige, H., Aotani, D., Fujisawa, T., Masuzaki, H., Hosoda, K., and Nakao, K. (2009) Beneficial effects of leptin on glycaemic and lipid control in a mouse model of type 2 diabetes with increased adiposity induced by streptozotocin and a high fat diet. *Diabetologia* **52,** 675–683
9. Ebihara, K., Kusakabe, T., Hirata, M., Masuzaki, H., Miyanaga, F., Kobayashi, N., Tanaka, T., Chusho, H., Miyazawa, T., Hayashi, T., Hosoda, K., Ogawa, Y., DePaoli, A. M., Fukushima, M., and Nakao, K. (2007) Efficacy and safety of leptin-replacement therapy and possible mechanisms of leptin actions in patients with generalized lipodystrophy. *J. Clin. Endocrinol. Metab.* **92,** 532–541
10. Farooqi, I. S., Jebb, S. A., Langmack, G., Lawrence, E., Cheetham, C. H., Prentice, A. M., Hughes, I. A., McCamish, M. A., and O'Rahilly, S. (1999) Effects of recombinant leptin therapy in a child with congenital leptin deficiency. *N. Engl. J. Med.* **341,** 879–884
11. Oral, E. A., Simha, V., Ruiz, E., Andewelt, A., Premkumar, A., Snell, P., Wagner, A. J., DePaoli, A. M., Reitman, M. L., Taylor, S. I., Gorden, P., and Garg, A. (2002) Leptin replacement therapy for lipodystrophy. *N. Engl. J. Med.* **346,** 570–578
12. Petersen, K. F., Oral, E. A., Dufour, S., Befroy, D., Ariyan, C., Yu, C., Cline, G. W., DePaoli, A. M., Taylor, S. I., Gorden, P., and Shulman, G. I. (2002) Leptin reverses insulin resistance and hepatic steatosis in patients with severe lipodystrophy. *J. Clin. Invest.* **109,** 1345–1350
13. Lee, Y., Hirose, H., Ohneda, M., Johnson, J. H., McGarry, J. D., and Unger, R. H. (1994) Beta-cell lipotoxicity in the pathogenesis of non-insulin-dependent diabetes mellitus of obese rats: impairment in adipocyte-beta-cell relationships. *Proc. Natl. Acad. Sci. U.S.A.* **91,** 10878–10882
14. Perseghin, G., Scifo, P., De Cobelli, F., Pagliato, E., Battezzati, A., Arcelloni,

C., Vanzulli, A., Testolin, G., Pozza, G., Del Maschio, A., and Luzi, L. (1999) Intramyocellular triglyceride content is a determinant of *in vivo* insulin resistance in humans. A ^{1}H-^{13}C nuclear magnetic resonance spectroscopy assessment in offspring of type 2 diabetic parents. *Diabetes* **48,** 1600–1606

15. Kim, J. K., Gavrilova, O., Chen, Y., Reitman, M. L., and Shulman, G. I. (2000) Mechanism of insulin resistance in A-ZIP/F-1 fatless mice. *J. Biol. Chem.* **275,** 8456–8460
16. Minokoshi, Y., Kim, Y. B., Peroni, O. D., Fryer, L. G., Müller, C., Carling, D., and Kahn, B. B. (2002) Leptin stimulates fatty-acid oxidation by activating AMP-activated protein kinase. *Nature* **415,** 339–343
17. Winder, W. W., Wilson, H. A., Hardie, D. G., Rasmussen, B. B., Hutber, C. A., Call, G. B., Clayton, R. D., Conley, L. M., Yoon, S., and Zhou, B. (1997) Phosphorylation of rat muscle acetyl-CoA carboxylase by AMP-activated protein kinase and protein kinase A. *J. Appl. Physiol.* **82,** 219–225
18. Andreelli, F., Foretz, M., Knauf, C., Cani, P. D., Perrin, C., Iglesias, M. A., Pillot, B., Bado, A., Tronche, F., Mithieux, G., Vaulont, S., Burcelin, R., and Viollet, B. (2006) Liver adenosine monophosphate-activated kinase-α2 catalytic subunit is a key target for the control of hepatic glucose production by adiponectin and leptin but not insulin. *Endocrinology* **147,** 2432–2441
19. Assifi, M. M., Suchankova, G., Constant, S., Prentki, M., Saha, A. K., and Ruderman, N. B. (2005) AMP-activated protein kinase and coordination of hepatic fatty acid metabolism of starved/carbohydrate-refed rats. *Am. J. Physiol. Endocrinol. Metab.* **289,** E794–E800
20. Shaw, R. J., Lamia, K. A., Vasquez, D., Koo, S. H., Bardeesy, N., Depinho, R. A., Montminy, M., and Cantley, L. C. (2005) The kinase LKB1 mediates glucose homeostasis in liver and therapeutic effects of metformin. *Science* **310,** 1642–1646
21. Moitra, J., Mason, M. M., Olive, M., Krylov, D., Gavrilova, O., Marcus-Samuels, B., Feigenbaum, L., Lee, E., Aoyama, T., Eckhaus, M., Reitman, M. L., and Vinson, C. (1998) Life without white fat. A transgenic mouse. *Genes Dev.* **12,** 3168–3181
22. Ogawa, Y., Masuzaki, H., Hosoda, K., Aizawa-Abe, M., Suga, J., Suda, M., Ebihara, K., Iwai, H., Matsuoka, N., Satoh, N., Odaka, H., Kasuga, H., Fujisawa, Y., Inoue, G., Nishimura, H., Yoshimasa, Y., and Nakao, K. (1999) Increased glucose metabolism and insulin sensitivity in transgenic skinny mice overexpressing leptin. *Diabetes* **48,** 1822–1829
23. German, J., Kim, F., Schwartz, G. J., Havel, P. J., Rhodes, C. J., Schwartz, M. W., and Morton, G. J. (2009) Hypothalamic leptin signaling regulates hepatic insulin sensitivity via a neurocircuit involving the vagus nerve. *Endocrinology* **150,** 4502–4511
24. Pocai, A., Obici, S., Schwartz, G. J., and Rossetti, L. (2005) A brain-liver circuit regulates glucose homeostasis. *Cell Metab.* **1,** 53–61
25. Davies, S. P., Carling, D., Munday, M. R., and Hardie, D. G. (1992) Diurnal rhythm of phosphorylation of rat liver acetyl-CoA carboxylase by the AMP-activated protein kinase, demonstrated using freeze-clamping. Effects of high fat diets. *Eur. J. Biochem.* **203,** 615–623
26. Miyamoto, L., Toyoda, T., Hayashi, T., Yonemitsu, S., Nakano, M., Tanaka, S., Ebihara, K., Masuzaki, H., Hosoda, K., Ogawa, Y., Inoue, G., Fushiki, T., and Nakao, K. (2007) Effect of acute activation of 5′-AMP-activated protein kinase on glycogen regulation in isolated rat skeletal muscle. *J. Appl. Physiol.* **102,** 1007–1013
27. Lee, Y., Yu, X., Gonzales, F., Mangelsdorf, D. J., Wang, M. Y., Richardson, C., Witters, L. A., and Unger, R. H. (2002) PPARα is necessary for the lipopenic action of hyperleptinemia on white adipose and liver tissue. *Proc. Natl. Acad. Sci. U.S.A.* **99,** 11848–11853
28. Brabant, G., Müller, G., Horn, R., Anderwald, C., Roden, M., and Nave, H. (2005) Hepatic leptin signaling in obesity. *FASEB J.* **19,** 1048–1050
29. Dzamko, N. L., and Steinberg, G. R. (2009) AMPK-dependent hormonal regulation of whole-body energy metabolism. *Acta Physiol.* **196,** 115–127
30. Uotani, S., Abe, T., and Yamaguchi, Y. (2006) Leptin activates AMP-activated protein kinase in hepatic cells via a JAK2-dependent pathway. *Biochem. Biophys. Res. Commun.* **351,** 171–175
31. Uyama, N., Geerts, A., and Reynaert, H. (2004) Neural connections between the hypothalamus and the liver. *Anat. Rec. A Discov. Mol. Cell. Evol. Biol.* **280,** 808–820
32. Hutchinson, D. S., and Bengtsson, T. (2006) AMP-activated protein kinase activation by adrenoceptors in L6 skeletal muscle cells. Mediation by α1-adrenoceptors causing glucose uptake. *Diabetes* **55,** 682–690
33. Xu, M., Zhao, Y. T., Song, Y., Hao, T. P., Lu, Z. Z., Han, Q. D., Wang, S. Q., and Zhang, Y. Y. (2007) α1-adrenergic receptors activate AMP-activated protein kinase in rat hearts. *Sheng Li Xue Bao* **59,** 175–182
34. Koh, H. J., Hirshman, M. F., He, H., Li, Y., Manabe, Y., Balschi, J. A., and Goodyear, L. J. (2007) Adrenaline is a critical mediator of acute exercise-induced AMP-activated protein kinase activation in adipocytes. *Biochem. J.* **403,** 473–481
35. Barnes, B. R., Ryder, J. W., Steiler, T. L., Fryer, L. G., Carling, D., and Zierath, J. R. (2002) Isoform-specific regulation of 5′-AMP-activated protein kinase in skeletal muscle from obese Zucker (fa/fa) rats in response to contraction. *Diabetes* **51,** 2703–2708
36. Bergeron, R., Previs, S. F., Cline, G. W., Perret, P., Russell, R. R., 3rd, Young, L. H., and Shulman, G. I. (2001) Effect of 5-aminoimidazole-4-carboxamide-1-β-D-ribofuranoside infusion on *in vivo* glucose and lipid metabolism in lean and obese Zucker rats. *Diabetes* **50,** 1076–1082
37. Yu, X., McCorkle, S., Wang, M., Lee, Y., Li, J., Saha, A. K., Unger, R. H., and Ruderman, N. B. (2004) Leptinomimetic effects of the AMP kinase activator 5-aminoimidazole-4-carboxamide 1-β-D-ribofuranoside (*AICAR*) in leptin-resistant rats: prevention of diabetes and ectopic lipid deposition. *Diabetologia* **47,** 2012–2021
38. Cool, B., Zinker, B., Chiou, W., Kifle, L., Cao, N., Perham, M., Dickinson, R., Adler, A., Gagne, G., Iyengar, R., Zhao, G., Marsh, K., Kym, P., Jung, P., Camp, H. S., and Frevert, E. (2006) Identification and characterization of a small molecule AMPK activator that treats key components of type 2 diabetes and the metabolic syndrome. *Cell Metab.* **3,** 403–416

INTERNAL MEDICINE

□ CASE REPORT □

Premature Atherosclerosis in a Japanese Diabetic Patient with Atypical Familial Partial Lipodystrophy and Hypertriglyceridemia

Masanori Iwanishi[1], Ken Ebihara[2], Toru Kusakabe[2], Shinji Harada[1], Jun Ito-Kobayashi[1], Atsushi Tsuji[3], Kiminori Hosoda[2] and Kazuwa Nakao[2]

Abstract

We herein report a case of premature atherosclerosis in a patient with familial partial lipodystrophy (FPL), diabetes mellitus, hypertension and hypertriglyceridemia. Sequencing of the candidate genes *LMNA*, *PPARG* and *CAV1* associated with FPL revealed no genetic abnormalities, which indicated the activity of a novel gene in this patient. The patient's son showed milder fat loss and similar fat distribution compared to the proband; however, the son showed no signs of any atherosclerotic disease. Although a cluster of atherogenic risk factors is likely to be the primary causes of atherosclerosis in our patient, other factors, including an unknown gene associated with FPL, the severity of fat loss and gender, might affect the development of atherosclerosis.

Key words: familial partial lipodystrophy (FPL), premature atherosclerosis, insulin resistance, pioglitazone

(Intern Med 51: 2573-2579, 2012)
(DOI: 10.2169/internalmedicine.51.7461)

Introduction

Lipodystrophies are a heterogeneous group of diseases characterized by generalized or partial fat loss (1-5). Some patients with partial lipodystrophies show fat hypertrophy in other locations. Lipodystrophy is diagnosed on the basis of fat loss in portions of the body determined with dual energy X-ray absorptiometry (DEXA) and magnetic resonance imaging (MRI) scans. Lipodystrophies are rare and have both inherited and acquired forms. Acquired lipodystrophies can be generalized or partial. Although the causes of acquired lipodystrophies are generally unknown, such acquired lipodystrophies can be associated with signs of autoimmunity. Patients with lipodystrophies often also have a cluster of associated diseases, including insulin resistance, dyslipidemia, hypertension, fatty liver and diabetes, similar to that observed in patients with metabolic syndrome. These patients often die of health problems, including ischemic heart disease, cerebral infarction, renal failure, severe liver dysfunction and pancreatitis. Congenital generalized lipodystrophies (CGLs) are autosomal recessive disorders that, in most patients, result from mutations in the genes encoding Seipin and 1-acylglycerol-3-phosphate-O-acyltransferase 2 (AGPAT2) (6). Familial partial lipodystrophies (FPLs) are autosomal dominant disorders, and mutations in the genes encoding laminin A/C, peroxisome proliferator-activated receptor-γ (PPARG) or caveolin have been reported in patients with FPL. Familial partial lipodystrophy, Dunnigan variety (FPLD) is named after Dunnigan, who provided a detailed description of the syndrome (7). FPLD is associated with several mutations in the genes encoding laminin A/C. However, a number of patients with FPL remain undiagnosed at the genetic level.

Women with FPLD have a higher prevalence of diabetes and atherosclerotic vascular disease, higher serum triglyceride (TG) levels and lower high-density lipoprotein (HDL) cholesterol concentrations than men with FPLD (3, 9). However, some patients with CGL or FPL do not have overt atherosclerotic diseases. Furthermore, the evidence for pre-

[1]Diabetes and Endocrine Division, Kusatsu General Hospital, Japan, [2]Department of Medicine and Clinical Science, Kyoto University Graduate School of Medicine, Japan and [3]Department of Neurosurgery, Kusatsu General Hospital, Japan
Received for publication February 8, 2012; Accepted for publication June 7, 2012
Correspondence to Dr. Masanori Iwanishi, masa-iwani@solid.ocn.ne.jp

Table 1. Biochemical Data of This Family

Metabolic variables		Patient 1	Patient 2	Normal values	
Plasma glucose		154	86	70-109	(mg/dL)
HbA1c		6.5	4.8	4.3-5.8	(%)
plasma insulin			5.6	2.2-12.4	(μU/mL)
plasma CPR		2.0		0.7-3.5	(ng/dL)
Serum triglycerides		755	125	35-149	(mg/dL)
Serum cholesterol		211	151	130-219	(mg/dL)
Serum HDL cholesterol		34	40	40-83	(mg/mL)
Serum leptin		36.1	3.9		(ng/mL)
Serum adiponectin		7.1	5.7		(μg/mL)
Urinary CPR	2003	68.7			(μg/day)
	2005	74.8			
	2007	10			

mature atherosclerosis in patients with CGL or other forms of FPL is minimal, probably because the number of patients with these conditions is small. The mechanisms underlying the development of atherosclerosis in patients with FPL remain unknown. Therefore, in this case report, we include the clinical findings and results of a genetic analysis for our patient in order to clarify the mechanisms underlying atherosclerosis in FPL.

Case Report

The patient was a 48-year-old woman. When she was 16 years old, she had a body mass index (BMI) of 36.5, which indicated obesity. At 35 years of age, she was diagnosed with diabetes by a family doctor based on the presence of high levels of hemoglobin A1c (HbA1c) and postprandial glucose. Her diabetes remained uncontrolled (HbA1c level: 8.0%-12.0%) despite treatment with a combination of 10 mg of glibenclamide and 0.6 mg of voglibose. At 40 years of age, she was transferred to the hospital emergency room due to convulsions and a disturbance of consciousness. Her magnetic resonance imaging (MRI, left panel) and magnetic resonance angiography (MRA, right panel) findings showed severe narrowing at the end of the internal carotid artery on both sides with an old cerebral infarction in the right anterior lobe (Fig. 3A, B). The narrowing in the proximal region of the anterior and middle cerebral arteries on both sides is indicated by arrows. The presence of lesions suggested a diagnosis of premature atherosclerosis, because the patient had multiple atherogenic risk factors, including diabetes mellitus, hypertension and hypertriglyceridemia. However, we could not completely rule out moyamoya disease, because we did not perform a biopsy of the lesions that narrowed the arterial wall (10). We initiated treatment with 160 mg of valsartan and 40 mg of Adalat-CR for hypertension in 2003 when the patient was 43 years old. Her blood pressure was reduced to 130/50 mmHg. Subsequently, superficial temporal artery-middle cerebral artery (STA-MCA) anastomosis was performed. The patient was admitted to our hospital for diabetes care in May 2007 when she was 48 years old. At that time, her height was 152 cm and she weighed 64 kg, which indicated a body mass index of 27.2. She did not have a history of either autoimmune or infectious diseases. She did not have a habit of smoking or consuming alcohol. She had entered menopause at the age of 40. Her HbA1c concentration was 6.5% (Table 1) and although her blood glucose level was found to be satisfactory on her first visit to our hospital, her dose of insulin was increased to 72 U/day (1.1 U/kg/day). Her serum TG level was 755 mg/dL and her HDL cholesterol level was 34 mg/dL; however, her blood glucose level was well-controlled. This suggested that the hypertriglyceridemia was due to insulin resistance. The patient did not have any other abnormal endocrinological findings, including abnormal cortisol levels. Her serum leptin level was 36.1 ng/mL, while her serum adiponectin level was 7.1 μg/mL. Her urinary C peptide level was 68.7 μg/day in 2003, 74.8 μg/day in 2005 and 10 μg/day in 2007. This observation indicated a recent deterioration in insulin deficiency despite the relatively conserved insulin levels observed in 2003 and 2005. The patient had mild nonproliferative diabetic retinopathy. Her total urinary protein level was 1.0 g/day and her serum creatinine level was 1.06 mg/dL, which indicated overt diabetic nephropathy. An abdominal echo showed mild fatty liver and the L/S ratio of the computed tomography (CT) value was 1.3. The patient's serum albumin level, platelet count and hyaluronic acid level were within normal limits, which suggested that she did not have severe non-alcoholic steatosis hepatitis. She had noticed a loss of subcutaneous fat over her forearms, lower limbs and buttocks at 12 years of age. On admission, she showed loss of subcutaneous fat deposits in the forearms (right panel), lower limbs and buttocks, with prominent lower limb musculature and excess fat deposition around the face, neck and trunk (left panel, Fig. 1B). The patient's mother and son showed a similar distribution of fat atrophy and we therefore considered an autosomal dominant pattern of inheritance (Fig. 1A). The patient's condition was clinically diagnosed as FPL. The patient's mother was diagnosed with diabetes at 31 years of age and died of a cerebral infarction at 38 years of age. The patient's father died of chronic renal failure at the age of 75 and was not evaluated for fat atrophy or glucose tolerance. We assessed body fat distribution in the proband (Patient 1) in 2007 using DEXA and MRI studies. Thoracic (left panel) and abdominal MRI (right panel) revealed preservation of subcutaneous fat in the abdominal and thoracic regions (Fig. 2A). MRI images obtained at the level of the gluteal fat revealed a marked loss of gluteal subcutaneous fat (Fig. 2B). Axial MRI performed at the level of the thigh (upper panel) and calf (lower panel) revealed a marked loss of subcutaneous fat in these regions (Fig. 2C). Patient 1 had decreased amounts of subcutaneous fat, particularly in the antero-lateral and posterior thigh and calf regions. Axial MRI performed at the level of the forearms (lower panel) revealed almost a complete absence of subcutaneous fat in the forearms, while axial MRI performed at the level of the arms (upper panel) revealed the preservation of subcutaneous fat in this region (Fig. 2D).

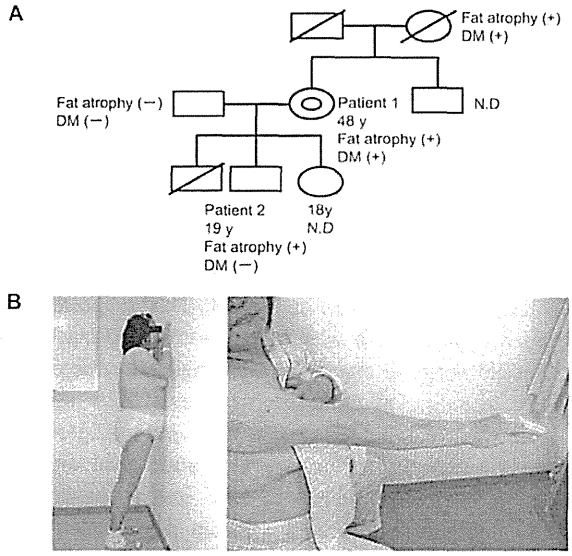

Figure 1. A. The pedigree of a Japanese family with lipodystrophy. While the proband (Patient 1) and her mother exhibited marked losses of subcutaneous fat in the lower limbs and buttocks, the son (Patient 2) exhibited only a moderate loss of subcutaneous fat. The proband and her mother both had diabetes mellitus. B. The phenotypic features of Patient 1 are shown in the left panel. Note the prominent musculature of the lower limbs as well as the preservation of abdominal and cervical fat and the loss of fat in the lower limbs and gluteal tissues. The right panel shows fat atrophy in the forearms and conservation of subcutaneous fat in the arms.

The area of visceral fat located at the umbilical level measured 140.4 cm^2. The regional and whole-body adipose tissue distribution and body composition estimated by the DEXA scan is shown in Table 2. Compared to normal subjects, Patient 1 had markedly lower levels of fat in her legs, with prominent accumulation of fat in the trunk. She appeared to have well-preserved skeletal muscle.

The son of Patient 1 (Patient 2) was a 19-year-old man. His height was 163 cm and weight was 86.8 kg, thus suggesting a body mass index of 32.7. His blood pressure showed a normal range, and he did not have any health problems except for obesity. We assessed fat atrophy in various regions in Patient 2 using a DEXA scan and CT. As shown in Table 2, we evaluated fat mass compared with two controls. The average BMI in Control Group 2, which included 72 healthy men between the ages of 20 and 29, was 22.4, while that in Control Group 3, which included 11 healthy men between the ages of 20 and 29, was 26.4. The finding of a BMI in Patient 2 of 32.7 kg/m^2 indicated that % fat and fat mass in one leg was relatively low, which suggested fat atrophy in the legs. The CT images of Patient 2 showed relatively low levels of subcutaneous fat in the thigh and buttocks (Fig. 4). Patient 2 had a marked loss of subcutaneous fat, particularly in the lateral thigh, calf and forearm regions. Patients with FPL show marked losses of subcutaneous fat, particularly in the lateral thigh and calf regions (3). Therefore, the fat distribution pattern observed in Patient 2 seemed to be similar to that of his mother (Patient 1) and was consistent with the above observations. The area of visceral fat located at the umbilical level measured 69.5 cm^2. Patient 2's fasting serum TG level was 125 mg/dL and his HbA1c level was 4.8%, both of which were within normal limits. An oral glucose tolerance test (OGTT) showed that Patient 2's blood glucose levels were 86, 111, 133 and 118 mg/dL, while his insulin levels were 5.6, 36.2, 92.9 and 68.8 μU/mL at 0, 30, 60 and 120 minutes. Therefore, the OGTT showed normal glucose levels with relatively high insulin levels. Both brain MRI and MRA showed normal results (data not shown). Therefore, Patient 2 did not have visceral obesity, hypertriglyceridemia, diabetes mellitus, hypertension or premature atherosclerosis, although he seemed to have partial lipodystrophy.

We examined the effects of pioglitazone on the metabolic values and the changes in lean mass and fat mass regions in Patient 1. We prescribed pioglitazone (15 mg/day) because thiazolidinediones have been reported to be effective for glycemic control in patients with FPL. We examined Patient 1's response to pioglitazone by monitoring her HbA1c levels and the changes in her biochemical data, body weight, fat and lean mass during treatment using DEXA. After three months of treatment, Patient 1's HbA1c level decreased from 9.2% to 7.1% and remained at approximately 7.0% thereafter, while her serum TG level decreased from 1,102 mg/dL to 431 mg/dL. After two weeks of pioglitazone treatment, the dose of insulin was reduced to 18 U/day (0.26 U/kg/day). After three months, Patient 1's body weight increased from 67.0 to 78.0 kg. We decreased the dose of pioglitazone to 7.5 mg to prevent additional gains in body weight. The changes in fat and lean mass were monitored during pioglitazone treatment using DEXA scans. In addition, we evaluated the changes in the leptin and adiponectin levels during pioglitazone treatment. A comparison of the results of the DEXA scans showed that the fat mass increased by 2.6 kg, while the lean mass increased by 6.5 kg during pioglitazone treatment. Pioglitazone induced increases in fat mass predominantly in the trunk, and no increases were detectable in the lower limbs. After three months of treatment, the serum adiponectin level increased from 7.1 to 24.0 μg/mL and the HDL cholesterol level increased from 34 mg/dL to 45 mg/dL.

We examined the sequences of the entire coding region and the exon-intron boundary regions of the *LMNA*, *PPARG* and *CAV1* genes, which are known to be associated with FPL; however, we found no mutations in these genes in the proband.

Discussion

We herein report the case of a 48-year-old Japanese woman (Patient 1) with diabetes and atypical FPL who showed marked losses of subcutaneous fat in the forearms, lower limbs and buttocks. The fat distribution pattern ob-

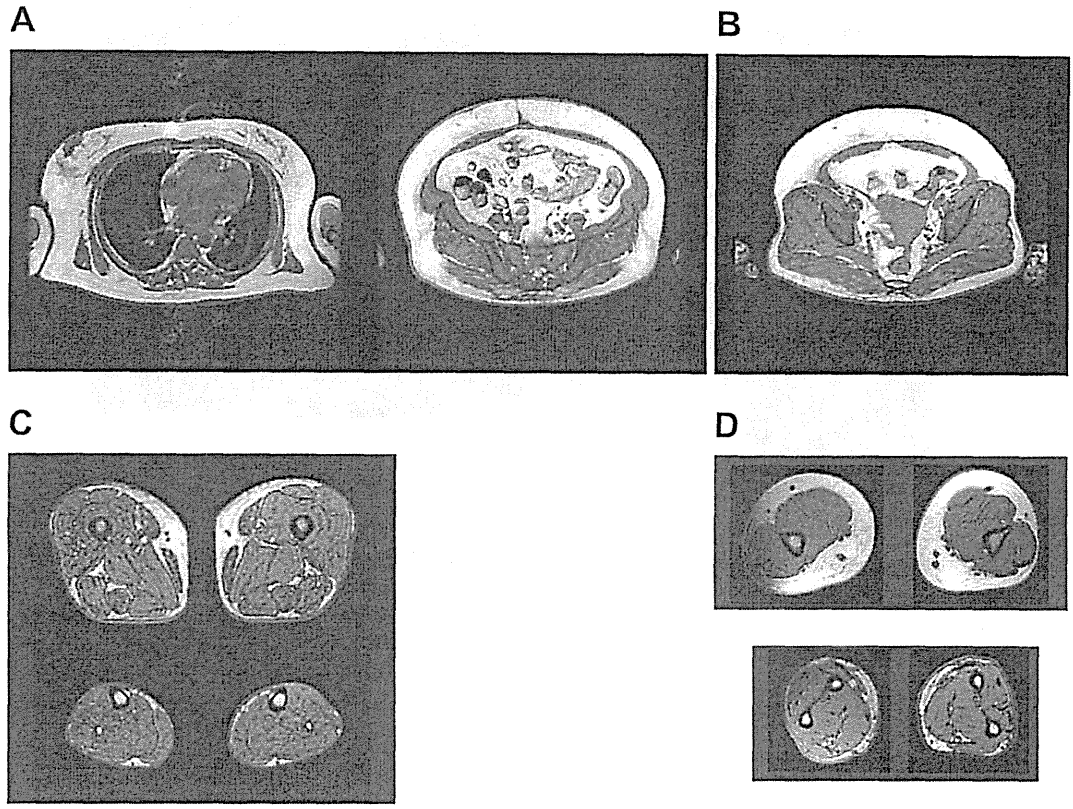

Figure 2. The figure shows magnetic resonance imaging (MRI) results for Patient 1. A. Thoracic MRI images taken at the level of the fourth thoracic vertebrae (left panel) and abdominal MRI images taken at the umbilical level (right panel) showed the preservation of subcutaneous fat in the thoracic and abdominal regions. B. A T1-weighted MRI image taken at the level of the gluteal fat indicated a striking loss of gluteal subcutaneous fat. C. MRI images taken at the level of the thigh (upper panel) and calf (lower panel) revealed a nearly complete absence of subcutaneous fat. Patient 1 had decreased amounts of subcutaneous fat, particularly in the antero-lateral and posterior thigh and calf regions. D. MRI images taken at the level of the arms (upper panel) and forearms (lower panel) revealed a marked loss of subcutaneous fat in the forearms and preservation of fat in the arms.

served in Patient 1 seemed to be similar to that seen in patients with atypical partial lipodystrophy with *PPARG* mutations (11-13).

Patient 1 had been severely obese since 16 years of age. Her abdominal CT images showed visceral obesity. The age of onset of diabetes mellitus in Patient 1 was 35 years, which was relatively early compared to that observed in patients with type 2 diabetes mellitus. At 40 years of age, Patient 1 showed severe narrowing at the end of the internal carotid artery on both sides with an old cerebral infarction in the right anterior lobe, which suggested the presence of premature atherosclerosis. Because Patient 1 had visceral obesity and FPL, her intra-hepatic and intra-myocellular lipid contents may have been increased, which may have caused greater insulin resistance and worsened the atherosclerosis. The serum adiponectin levels are thought to be associated with the indices of insulin resistance and atherosclerosis (14, 15). Patient 1's serum adiponectin level was 7.1 μg/mL. The data suggested that Patient 1's serum adiponectin levels were relatively lower than those in 28 women with normal glucose tolerance (16). The level of adiponectin may also have had an effect on atherosclerosis in the case of Patient 1. Women with FPLD have a higher prevalence of diabetes and atherosclerotic vascular disease, higher serum TG levels and lower HDL cholesterol concentrations than men with FPLD (3, 9). Therefore, because Patient 1 was a woman with FPL and had a cluster of atherogenic risk factors, including diabetes mellitus, hypertension and hypertriglyceridemia, she had a predisposition for developing atherosclerosis. On the other hand, her son did not have premature atherosclerosis. The reasons for this were thought to be as follows: first, Patient 1's son was a 19-year-old man with a less severe amount of fat loss compared to his mother; second, he did not have hypertriglyceridemia, hypertension or diabetes mellitus, although he did have insulin resistance. We previously reported the case of a Japanese woman with diabetes with atypical FPL who had normal serum TG levels and did not have overt atherosclerosis (17).

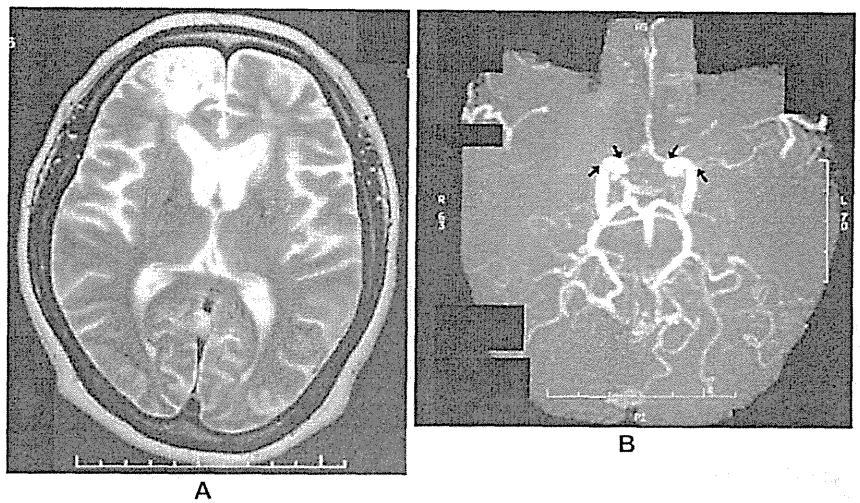

Figure 3. Brain magnetic resonance imaging (MRI), which had been performed when Patient 1 was transferred to the emergency room for convulsions at 40 years of age, showed an old infarction in the right frontal lobe (left panel), while brain magnetic resonance angiography (MRA) showed severe narrowing in the end of both sides of the internal carotid artery (right panel). The narrowing in the proximal region of both sides of the anterior cerebral and middle cerebral arteries is indicated by arrows.

Table 2. Body Composition as Determined by DEXA Scan in the Patient 1 and the Patient 2

	Patient 1	Control 1	Patient 2	Control 2	Control 3
Height (cm)	152.0	156.1 ± 4.9	163.0	172.2 ± 5.3	170.4 ± 4.0
Body weight (kg)	69.0	55.1 ± 6.7	86.8	66.4 ± 9.9	80.4 ± 8.7
BMI (kg/m^2)	30.0	22.7 ± 3.0	32.7	22.4 ± 3.2	27.7 ± 2.6
Age (years)	48	45.1 ± 2.8	19	25.6 ± 2.7	26.4 ± 1.8
1) Fat (%)					
whole body	31.6	30.3 ± 6.2	25.7	15.6 ± 9.5	25.6 ± 6.2
one arm	46.4	26.9 ± 7.3	30.6	11.9 ± 5.9	20.1 ± 6.4
one leg	15.4	33.2 ± 5.7	20.3	16.3 ± 6.4	25.0 ± 5.6
trunk	37.9	28.4 ± 7.7	27.9	15.7 ± 8.3	27.3 ± 7.3
2) Fat Mass (kg)					
whole body	23.8	16.8 ± 5.2	19.3	10.8 ± 6.4	20.7 ± 6.8
one arm	1.5	0.7 ± 0.3	1.6	0.4 ± 0.3	0.8 ± 0.3
one leg	1.1	3.5 ± 1.0	2.7	2.2 ± 1.1	3.9 ± 1.1
trunk	15.0	7.1 ± 2.8	10.8	4.8 ± 3.4	10.0 ± 4.0
3) Lean Mass (kg)					
whole body	49.0	35.3 ± 3.1	53.7	52.0 ± 5.4	55.5 ± 0.2
one arm	1.7	1.7 ± 0.2	3.5	2.7 ± 0.4	2.9 ± 0.3
one leg	5.9	6.6 ± 0.9	10.0	10.2 ± 1.6	10.9 ± 1.4
trunk	23.9	16.3 ± 1.3	27.3	22.7 ± 2.3	24.6 ± 2.5

※ *Normal values in control 1 are obtained from 55 healthy women between the ages of 40 years and 49 years. Normal values in control 2 are obtained from 72 healthy men between the ages of 20 years and 29 years, while ones in control 3 are obtained from 11 healthy men between ages of 20 years and 29 years. Fat(%), Fat mass and Lean mass in one arm and leg indicates the mean values of left and right arm (or leg).*

Therefore, the severity of atherosclerosis in women with FPL seems to be variable, although the evidence for accelerated atherosclerosis in patients with FPL is minimal.

Hegele RA has also reported FPLD with the *LMNA* codon 482 mutation to be associated with an increased risk of developing early coronary heart disease (8). In that report, the author speculated that *LMNA* mutations within arterial walls may affect the progression of atherosclerosis. In addition, we can speculate that an unidentified gene may affect arterial walls, which may have accelerated the progression of atherosclerosis in the case of Patient 1.

Dyslipidemia is common in insulin resistance and is characterized by fasting hypertriglyceridemia, low levels of HDL cholesterol and a delayed clearance of TG-rich lipoproteins, including very low density lipoproteins (VLDLs) (18, 19). Recently, the mechanisms underlying the development of hypertriglyceridemia in patients with general and partial lipodystrophies have been reported (20, 21). Hepatic VLDL

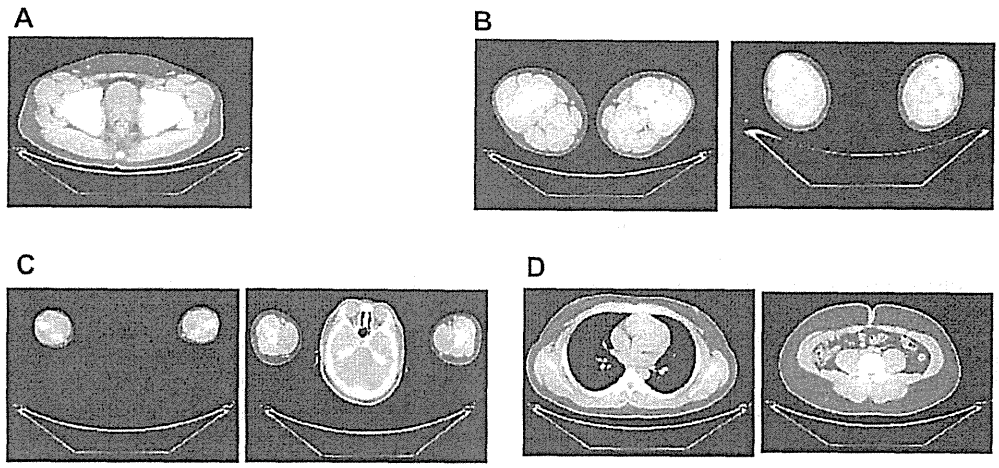

Figure 4. Computed tomography (CT) images of various regions of the patient's son (Patient 2) were obtained to evaluate fat distribution. A. CT images taken at the level of the gluteal fat were obtained. B. CT images taken at the level of the thigh are shown in the left panel, while images taken at the level of the calf are shown in the right panel. Patient 2 had decreased amounts of subcutaneous fat, particularly in the lateral thigh and calf regions. C. CT images taken at the level of the forearms are shown in the left panel, while images taken at the level of the arms are shown in the right panel. Patient 2 had decreased amounts of subcutaneous fat, particularly in the lateral forearms. D. Thoracic CT images taken at the level of the fourth thoracic vertebrae are shown in the left panel, while abdominal CT images taken at the umbilical level are shown in the right panel.

production increases in patients with insulin resistance and partial lipodystrophy. In the case of Patient 1, the serum levels of fasting TG, apolipoprotein C2, C3 and E were high (data not shown), which indicated a high concentration of VLDLs in the blood. Such high levels of VLDLs cause increases in *de novo* lipogenesis in the liver. Therefore, the presence of VLDL remnants may be the primary cause of accelerated atherosclerosis in Patient 1.

Although the effects of thiazolidinediones on glycemic control appear to vary in patients with FPL (11, 17, 22-26), pioglitazone treatment decreased the levels of HbA1c and fasting TG in the case of Patient 1. It is conceivable that pioglitazone improves glycemic control and triglycemic control by reducing the levels of free fatty acids (FFA) in venous effluent from adipose tissue and by limiting the lipotoxicity of other insulin-sensitive tissues, e.g. the liver and muscle (27, 28). In Patient 1, pioglitazone not only increased fat mass, but also increased lean mass. Although the significance of increased lean mass is not known, we might speculate that pioglitazone improves glycemic control not only by inducing adipocyte differentiation, but also by increasing the lean mass.

In conclusion, we herein described a case of premature atherosclerosis in a Japanese diabetic patient with atypical FPL and hypertriglyceridemia. Pioglitazone was effective in controlling the blood glucose levels, TG and adiponectin. In this case, the sequencing of candidate genes *LMNA*, *PPARG* and *CAV1*, which are known to be associated with FPL, revealed no genetic abnormalities and therefore suggested that a novel gene may be involved. Although a cluster of atherogenic risk factors in a woman with FPL is likely to play a major role in atherosclerosis, other factors, including genes associated with FPL, might affect the development of atherosclerosis. Further studies should be performed in order to obtain additional clinical and genetic information to better understand the mechanisms underlying premature atherosclerosis in patients with FPL.

The authors state that they have no Conflict of Interest (COI).

Acknowledgement

We thank Dr Takashi Shiokawa (Tanita Inc, Tokyo, Japan) for providing the DEXA data of 55 healthy women between the ages of 40 and 49, and of 72 healthy men between the ages of 20 and 29.

References

1. Semple RK, Krishna V, Chatterjee K, O'Rahilly S. PPARG and human metabolic disease. J Clin Invest **116**: 581-589, 2006.
2. Agarwal AK, Garg A. Genetic disorders of adipose tissue development, differentiation and death. Annu Rev Genomics Hum Genet **7**: 175-199, 2006.
3. Agarwal AK, Garg A. Genetic basis of lipodystrophies and management of metabolic complications. Annu Rev Med **57**: 297-311, 2006.
4. Kim SK, Park SW, Hwang IJ, Lee YK, Cho YW. High fat stores in ectopic compartments in men with newly diagnosed type 2 diabetes: an anthropometric determinant of carotid atherosclerosis and insulin resistance. International Journal of Obesity **34**: 105-110, 2010.
5. Garg A. Lipodystrophies: Genetic and acquired body fat disorders. J Clin Endocrinol Metab **96**: 3313-3325, 2011.

6. Ebihara K, Kusakabe T, Masuzaki H, et al. Genes and phenotype analysis of congenital generalized lipodystrophy in Japanese: a novel homozygous nonsense mutation in seipin gene. J Clin Endocrinol Metab **89**: 2360-2364, 2004.
7. Dunnigan MG, Cochrane MA, Kelly A, Scott JW. Familial lipoatrophic diabetes with dominant transmission. Quarterly Journal of Medicine **169**: 33-48, 1974.
8. Hegele RA. Premature atherosclerosis associated with monogenic insulin resistance. Criculation **103**: 2225-2229, 2001.
9. Garg A. Gender differences in the prevalence of metabolic complications in familial partial lipodystrophy (Dunnigan variety). J Clin Endocrinol Metab **85**: 1776, 2000.
10. Pollak L. Mayamoya disease and moyamoya syndrome. N Engl J Med **260**: 1226-1237, 2009.
11. Savage DB, Tan GD, Acerini CL, et al. Human metabolic syndrome resulting from dominant-negative mutations in the nuclear receptor peroxisome proliferator-activated receptor-G. Diabetes **52**: 910-917, 2003.
12. Hegele RA, Cao H, Frankowski C, Mathews S, Leff T. PPARG F 388L, a transactivation-deficient mutant, in familial partial lipodystrophy. Dabetes **51**: 3586-3590, 2002.
13. Agarwal AK, Grag A. A novel heterozygous mutation in peroxisom proliferator-activates receptor-G gene in a patient with familial partial lipodystrophy. J Clin Endorinol Metab **87**: 408-411, 2002.
14. Haque WA, Shimomura I, Matsuzawa Y, Garg A. Serum adiponectin and leptin levels in patients in patients with lipodystrophies. J Clin Endocrinol Metab **87**: 2395-2398, 2002.
15. Cook JR, Semple RK. Hypoadiponectinemia-cause or consequence of human insulin resistance? J Clin Endocrinol Metab **95**: 1544-1554, 2010.
16. Hotta K, Funahashi T, Arita Y, et al. Plasma concentrations of a novel, adipose-specific protein, adiponectin, in type 2 diabetic patients. Arterioscler Thromb Vasc Biol **20**: 1595-1599, 2000.
17. Iwanishi M, Ebihara K, Kusakabe T, et al. Clinical characteristics and efficacy of pioglitazone in a Japanese diabetic patient with an unusual type of familial partial lipodystrophy. Metabolism **58**: 1681-1687, 2009.
18. Ginsberg HN, Zhang YL, Hernandea-Ono A. Regulation of plasma triglycerides in insulin resistance and diabetes. Archives of Medical Research **36**: 232-240, 2005.
19. Adiel M, Taskinen MR, Boren J. Fatty liver, insulin resistance and dyslipidemia current diabetes reports. **8**: 60-64, 2008.
20. Simha V, Garg A. Inherited lipodystrophies and hypertriglyceridemia. Current Opinion in Lipodology **20**: 300-308, 2009.
21. Semple RK, Sleigh A, Murgatroyd PR, et al. Post receptor insulin resistance contributes to human dyslipidemia and hepatic steatosis. J Clin Invest **119**: 315-322, 2009.
22. Arioglu EA, Duncan-Morin J, Sebring N, et al. Efficacy and safety of troglitazone in the treatment of lipodystrophy syndromes. Ann Intern Med **133**: 263-274, 2000.
23. Owen KR, Donohoe M, Ellard S, Hattersley AT. Response to treatment with rosiglitazone in familial partial lipodystrophy due to a mutation in the LMNA gene. Diabet Med **20**: 823-827, 2003.
24. Sleilati GG, Leff T, Bonnett JW, Hegele R. Efficacy and safety of pioglitazone in treatment of a patient with an atypical lipodystrophy syndrome. Endocri Pract **13**: 656-661, 2007.
25. Ludtke A, Heckt K, Geneschel J, et al. Long-term treatment experience in a subject with Dunnigan-type familial partial lipodystrophy: efficacy of rosiglitazone. Diabet Med **22**: 1611-1613, 2005.
26. Gaudillat CC, Bancel AB, Beressi JP. Long-term improvement of metabolic control with pioglitazone in a woman with diabetes mellitus related to Dunigan syndrome: A case report. Diabetes Metab **35**: 151-154, 2009.
27. Majal KA, Cooper MB, Luc SG, Taskinen MR, Betteridge DJ. The effect of sensitization to insulin with pioglitazone on fasting and postprandial lipid metabolism, lipoprotein modification by lipases, and lipid transfer activites in type 2 diabetic patients. Diabetologia **49**: 527-537, 2006.
28. Ynag X, Smith U. Adipose tissue distribution and risk of metabolic disease: does thiazolidinedione-induced adipose tissue redistribution provide a clue to the answer? Diabetologia **50**: 1127-1133, 2007.